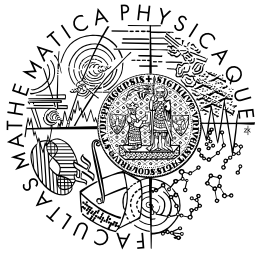

FACULTY
OF MATHEMATICS
AND PHYSICS
Charles University

BACHELOR THESIS

Peter Kottman

Jump conditions and dynamic surface tension at non-material interfaces

Mathematical Institute of Charles University

Supervisor of the bachelor thesis: RNDr. Ondřej Souček, Ph.D.

Study program: Physics (B1701)

Study branch: FOF (1701R026)

Prague 2021

I declare that I carried out this bachelor thesis independently, and only with the cited sources, literature and other professional sources. It has not been used to obtain another or the same degree.

I understand that my work relates to the rights and obligations under the Act No. 121/2000 Sb., the Copyright Act, as amended, in particular the fact that the Charles University has the right to conclude a license agreement on the use of this work as a school work pursuant to Section 60 subsection 1 of the Copyright Act.

In ..... date ....

Author's signature

Acknowledgements

The work presented in Chapter 2 was funded by the Charles University SFG grant program. I would like to thank the Faculty of Mathematics and Physics for supporting its students' first steps in academic research.

I would also like to thank the organizers of the *Introduction to FEniCS* masterclass organized by SIAM Student Chapter Prague for helping me with my first steps in finite element method and FEniCS.

Next, I am extremely grateful to my supervisor Dr. Ondřej Souček, not only for his patience and his guidance in the labyrinth of continuum mechanics, but also for his great musical recommendations. Thank you for having the courage to trust me with this subject!

Last but not least, I would like to thank my parents immensely for supporting the journey that led me here in every possible way. While the next few dozens of pages might be a result of a year of my work, it is just as much a result of twenty-three years of yours. So, mom, dad, if you find a mistake in here, the blame is to be shared...

Title: Jump conditions and dynamic surface tension at non-material interfaces

Author: Peter Kottman

Institute: Mathematical Institute of Charles University

Supervisor: RNDr. Ondřej Souček, Ph.D., Mathematical Institute of Charles University

Abstract: Problems involving fluid flow across phase interfaces arise in many branches of physics and engineering, making correct description of fluid behavior near an interface an important issue. In this thesis we study the quasi-static Stokes flow of a linearly viscous fluid, comparing two different jump conditions for traction. By reproducing the results from the relevant literature we motivate the assumption of nontrivial traction jump as the limit of the solution of governing equations across a transitional layer of finite thickness with the thickness going to zero, and we compare it to the classical traction continuity condition implied by the modified Reynolds transport theorem. The original method of derivation of the nontrivial traction jump involves manipulation of terms ill-defined even in the sense of distributions. To interpret these correctly, we use the Colombeau algebra of generalized functions. We derive the form of the traction jump for radially symmetric flow rigorously and show that this result is identical to the one obtained by the original method. The theoretical results are accompanied by numerical experiments, and possible generalizations as well as physical significance of the results are discussed.

Keywords: jump condition, phase interface, traction, Colombeau algebra, Stokes flow

Názov práce: Skokové podmienky a dynamické povrchové napätie na nemateriálových rozhraniach

Autor: Peter Kottman

Ústav: Matematický ústav UK

Vedúci bakalárskej práce: RNDr. Ondřej Souček, Ph.D., Matematický ústav UK

Abstrakt: Prúdenie tekutiny cez fázové rozhranie je súčasťou úloh mnohých odvetví fyziky a inžinierstva. Správny popis vývoja systému v blízkozti rozhrania teda hrá kľúčovú úlohu. V tejto bakalárskej práci sa zameriavame na stacionárne Stokesovské prúdenie lineárnej viskóznej tekutiny a porovnávame dve rôzne skokové podmienky pre trakčný vektor. Reprodukciou výsledkov v relevantnej literatúre motivujeme predpoklad netriviálneho skoku trakcie ako limitu riešení bilančných rovníc v prechodovej zóne konečnej šírky pre šírku zmenšujúcu sa k nule a porovnávame ho s klasickou podmienkou na spojitosť trakcie, ktorá vyplýva z modifikovanej Reynoldsovej vety o transporte. Pôvodná metóda odvodenia netriviálneho skoku trakcie pracuje s výrazmi, ktoré ani v distribúciách nie sú dobre definované. Na ich korektnú interpretáciu používame Colombeau algebru zovšeobecnených funkcií. V rámci nej formulujeme odvodenie skoku trakcie pre radiálne symetrické prúdenie a porovnaním s pôvodným odvodením hodnotíme, že je identické s výsledkami z literatúry. Teoretické výsledky ilustrujeme numerickými štúdiami a diskutujeme ich možné zovšeobecnenia ako aj fyzikálny význam dosiahnutých výsledkov.

Kľúčové slová: skoková podmienka, fázové rozhranie, trakcia, Colombeau algebra, Stokesovské prúdenie

List of Symbols and Abbreviations

Number Sets

$\overline{\mathbb{C}}$	generalized complex numbers
$\overline{\mathbb{C}}_0$	generalized complex numbers that have an associated usual complex number
$\mathbb{C}$	complex numbers
$\mathbb{N}$	natural numbers
$\mathbb{N}_0$	nonnegative integers
$\mathbb{R}$	real numbers

Vector Spaces

$\mathcal{D}$	infinitely differentiable functions with compact support
$\mathcal{D}'$	distributions
$\mathcal{G}$	Colombeau generalized functions
$\mathbb{R}^n$	n-dimensional Euclidean vector space
C^0	continuous functions
C^∞	infinitely differentiable functions
H^1	square-integrable functions with square-integrable weak first derivatives in the Lebesgue sense
L^2	square-integrable functions in the Lebesgue sense

Vector Analysis Operators

div	divergence
∇	gradient

Physical Quantities

$\mathbb{D}(\mathbf{v})$	symmetric part of the velocity gradient
$\mathbb{S}$	deviatoric part of the Cauchy stress tensor

η shear viscosity

λ bulk viscosity

Ψ stream function

ρ density

$\mathbb{T}$ Cauchy stress tensor

$\mathbf{v}$ Eulerian velocity of a fluid

$\mathbf{w}$ Eulerian velocity of a singular surface

Other Symbols

$\mathbb{I}$ identity tensor

$[\![f]\!]$ jump of the quantity f at singular surface

$\otimes$ dyadic (tensor) product

$\mathbf{e}_q$ unit vector in the direction of the coordinate q

Abbreviations

ODE ordinary differential equation

PDE partial differential equation

List of Figures

Contents

Introduction

Arguably the biggest scientific revolution of the 20^{th} century is the rise of quantum physics and the description of microscopic world it provides. However, the formalism of quantum physics becomes very impractical when it comes to describing systems on larger scales, and the numerical requirements of such approach tend to exceed the present computational possibilities. This is why classical physics is still relevant today for solving physical problems on mesoscopic and macroscopic scales. The classical theory of physical laws is used namely in problems of solid and fluid mechanics and thermodynamics.

That said, there exist physical systems whose description demands a cooperation of these two theories in order to obtain a *macroscopic* description of *microscopic* phenomena. A prime example of such situation is a system with a phase transition taking place. Although the microscopic description of a phase change alone can be given by statistical physics, if coupled with fluid flow for example, macroscopic description of the underlying phenomena is needed to study the evolution of this system. In more general terms, the medium-scale to large-scale systems are studied in the framework of *continuum mechanics*, where, as the name suggests, physical quantities are assumed to possess some regularity properties (e.g. continuity or continuous differentiability in the region occupied by the system). However, certain problems in continuum mechanics involve settings where one or more quantities are discontinuous across an *interface*, for example the phase interface mentioned above. Therefore, the question is how to model mechanical evolution of such systems.

This question has been treated in numerous publications over the last few decades, Anderson et al. [1998], Rajagopal and Tao [1995], and Slattery et al. [2007] to name just a few. The conventional method of working with flows across interfaces is to set up governing equations for homogeneous parts of the system and prescribe the assumed discontinuities of each relevant quantity in the form of a *jump condition*. One of the jump conditions that are usually postulated in these problems is the *continuity* of traction (normal component of the stress tensor) across the interface, as argued by Martinec [2010] for example.

However, there have been multiple hints that this condition might not lead to physically sensible results. In the context of Earth geophysics, Corrieu et al. [1995] and Ricard [2015] have made remarks on the *incompatibility of the traction continuity* assumption with the approach of solving the governing equations numerically inside the interface. Motivated by these remarks, Chambat et al. [2014] have proposed an alternative traction jump condition that is consistent with the so-called *diffuse interface* point of view. The paper by Chambat et al. [2014] proves the jump condition for the particular case of quasi-static Stokes flow

and illustrates its implications on systems with simple geometries.

Besides its obvious physical meaning, the diffuse interface is a very convenient tool in numerical simulations of fluid problems. The correct implementation and treatment of discontinuous quantities in floating point arithmetic can be quite difficult and the simplest solution is often to *regularize* the discontinuities and create a transitional layer as a numerical tool rather than a physical phenomenon in itself. Its use is probably the most prominent in the so-called *level set method* illustrated, e.g., by Lindbo [2006]. What Chambat et al. [2014] show in their paper is that this approach can lead to inconsistencies between the computed solutions and the expected physical behavior. As can be seen in Figure 1, taking a simple problem that can be solved analytically and comparing velocities for the sharp and diffuse interface models, it is evident that *the sharp interface with continuous traction is* ***not*** *the limit of the diffuse interface inside which the governing equations hold as the interface thickness goes to zero.* Instead, this limiting process leads to a discontinuity in traction across the interface, which Chambat et al. [2014] attribute to a new physical quantity named *dynamic surface tension.*

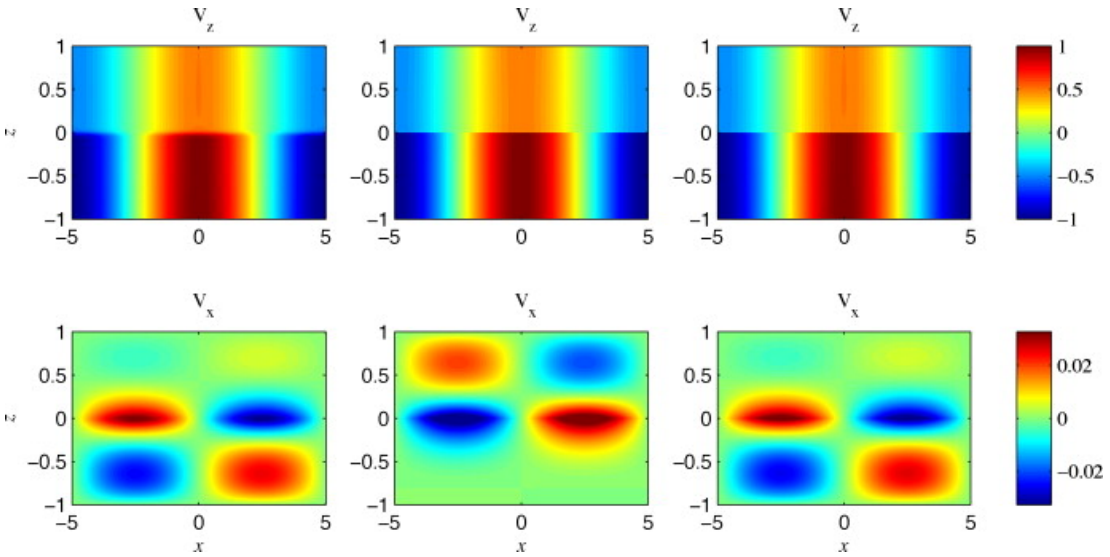

Figure 1: The z- and x-components of velocities in the quasi-static Stokes flow across an interface. The plots on the left correspond to the diffuse interface solution, whereas the middle pair of plots shows the solution of the sharp interface model with continuous traction. It is clear that despite the z-components of the velocity field being very similar for both solutions, the x-components differ considerably. The plots on the right show the sharp interface model with discontinuous traction and dynamic surface tension. The plots were taken from Chambat et al. [2014].

In the formal derivation of their jump condition, Chambat et al. [2014] have pointed out considerable difficulties in interpreting specific terms that arise in the governing equations. If the physical quantities describing the system are assumed discontinuous, the equations have to be solved in a *generalized* sense of distributions. However, the well-established linear theory of distributions is not suited to treatment of nonlinear operations, as was proved by Schwartz [1954]; and the governing equations of the system described by Chambat et al. [2014] contain several terms that would translate to a multiplication of two distributions. In

order to obtain a fully mathematically correct derivation of the new traction jump condition, an even broader theoretical toolkit is needed. This toolkit comes in the form of the *Colombeau algebra of generalized functions*, as found in a textbook by Rosinger [1987] for example. This mathematical framework has already been used in a similar context by Průša and Rajagopal [2016] to determine the response to a step input in nonlinear solid mechanics.

The aim of this thesis is to take a particular physical system with an interface that has relevant applications to the real-world setting despite being relatively simple. For this system, we shall reproduce and comment on existing results, namely the examples given by Chambat et al. [2014], to motivate the traction discontinuity assumption. Next, we shall derive these results in a more general mathematical setting, thus providing a rigorous interpretation of the jump condition proposed by Chambat et al. [2014], and we shall discuss possible implications for more complex systems. These results will then be illustrated numerically.

In Chapter 1, we introduce the notions in continuum mechanics pertinent to the subject of the thesis, such as the mechanical balance laws and description of interfaces, and we set up the model problem to be studied in the subsequent chapters.

Chapter 2 essentially motivates the work presented in the thesis by taking a simple physical system that can be resolved both analytically and numerically, and comparing the results obtained from different methods. The comparison leads to the introduction of a nontrivial traction jump condition described by dynamical surface tension. This chapter also serves as a reproduction of results published by Chambat et al. [2014].

Further insights into the nature of dynamic surface tension are given in Chapter 3. Two specific simple geometries with analytic diffuse interface solutions are considered, and we show how the limiting process of approximating the sharp interface by the diffuse interface leads to a jump in traction in these special cases.

Chapter 4 is devoted to the Colombeau algebra. First, we briefly review its construction and its properties. We then apply this generalized framework to our model problem to obtain an expression for the traction jump in a special one-dimensional case, which can be compared by the Chambat et al. [2014] traction jump. This theoretical result is also illustrated numerically, and the convergence of diffuse interface solutions to the sharp interface with dynamic surface tension is discussed in further detail.

Finally, Chapter 5 comments on possible generalizations of the model problem, outlining the issues that may arise when interpreting more general models via Colombeau algebra. Then, the physical significance of the effect caused by dynamic surface tension is addressed.

At the end of the thesis, two appendices are included. These contain detailed proofs of various mathematical properties used throughout the thesis and whose proofs, while fairly illustrative, would be considered tangents if placed inside the body of the thesis.

Chapter 1

Formulation of Mechanical Problems in Domains with Singular Surfaces

We start by presenting an overview of the concepts in continuum mechanics crucial to the main topic of this thesis. We first give a brief exposition of the balance laws used to describe the system evolution. Next, we introduce elementary and more advanced formal treatments of physical interfaces in continuous bodies. The chapter is concluded by the formulation of the quasi-static Stokes flow problem that will be referred to throughout subsequent chapters.

In continuum mechanics, there are two main mathematical descriptions of the studied system: *Lagrangian* and *Eulerian*. The former describes physical quantities with respect to the *reference configuration* of the continuous body and is more suited to solid mechanics, while the latter describes the system with respect to its *current configuration* and since it is more suitable for fluid mechanics, it is the one that we shall adopt from now on.

1.1 Balance Laws

The continuum mechanics theory consists of a specific mathematical description of a given macroscopic system and a set of physical principles that dictate its evolution. These are represented by *balance laws* that link the time evolution of certain quantities to other quantities and properties of the system. They are essentially interpretations of fundamental laws of classical mechanics and thermodynamics in the mathematical framework of continuum mechanics.

From a purely physical perspective, the laws of classical mechanics and thermodynamics are formulated in an *integral* sense. They prescribe the evolution or the expected properties of a system as a whole. However, the continuous approach calls for a description of the system that is *local* from a mathematical point of view. The connection between the global (volume) and the local (point-wise) forms of balance laws is made using the *Reynolds transport theorem*. It asserts that if ϕ is a continuously differentiable scalar or vector field defined in a material

(i.e. advected by the fluid) control volume $\omega(t)$ in the current configuration, then

$$\frac{\mathrm{d}}{\mathrm{d}t}\int_{\omega(t)}\phi\,\mathrm{d}x=\int_{\omega(t)}\left(\frac{\partial\phi}{\partial t}+\operatorname{div}\left(\phi\otimes\mathbf{v}\right)\right)\,\mathrm{d}x, \tag{1.1}$$

where $\mathbf{v}=\mathbf{v}(\mathbf{x},t)$ is the Eulerian velocity field, holds.[1] The proof of the theorem can be found, e.g., in a textbook by [Martinec, 2010, p. 42 – 44]. It uses the Gauss integration formulae that for a vector field $\mathbf{u}$ and a tensor field $\mathbb{A}$ read respectively

$$\int_{\omega}\operatorname{div}\mathbf{u}\,\mathrm{d}x=\int_{\partial\omega}\mathbf{u}\cdot\mathbf{n}\,\mathrm{d}s, \tag{1.2}$$

$$\int_{\omega}\operatorname{div}\mathbb{A}\,\mathrm{d}x=\int_{\partial\omega}\mathbb{A}\mathbf{n}\,\mathrm{d}s. \tag{1.3}$$

1.1.1 Mass and Momentum Balance Laws

The mass balance law states that *the mass of a continuous body is conserved*, i.e., it is the same at all times. In continuum mechanics, the mass is defined as a volume integral of the density field $\rho(\mathbf{x},t)$. The integral form of the mass balance can therefore be written as

$$\frac{\mathrm{d}}{\mathrm{d}t}\int_{\omega(t)}\rho\,\mathrm{d}x=0, \tag{1.4}$$

where $\omega(t)$ is an arbitrary control volume and $\frac{\mathrm{d}}{\mathrm{d}t}$ denotes the usual total time derivative.

If we then apply the Reynolds transport theorem (1.1) to the identity (1.4) and use the *localization lemma* (cf. Kopáček [2015]), we get the local mass balance equation

$$\frac{\partial\rho}{\partial t}+\operatorname{div}\left(\rho\mathbf{v}\right)=0. \tag{1.5}$$

The momentum balance is the continuum mechanics counterpart of *Newton's second law*. It relates the time evolution of system's momentum to the action of *body* and *contact* forces and can be expressed in its global form for a control volume $\omega(t)$ as

$$\frac{\mathrm{d}}{\mathrm{d}t}\int_{\omega(t)}\rho\mathbf{v}\,\mathrm{d}x=\int_{\omega(t)}\rho\mathbf{b}\,\mathrm{d}x+\int_{\partial\omega(t)}\mathbb{T}\mathbf{n}\,\mathrm{d}s. \tag{1.6}$$

Here $\mathbf{b}$ represents the density of body forces, $\mathbb{T}$ is the Cauchy stress tensor, and $\mathbf{n}$ denotes the unit outward normal to $\partial\omega(t)$.

As with the mass balance, the local momentum balance equation can be obtained using the Reynolds transport theorem and the localization lemma, as well as the Gauss integration formula (1.3). The resulting identity reads

$$\frac{\partial}{\partial t}(\rho\mathbf{v})+\operatorname{div}\left(\rho\mathbf{v}\otimes\mathbf{v}\right)=\rho\mathbf{b}+\operatorname{div}\mathbb{T}. \tag{1.7}$$

[1] If ϕ is a scalar field, then the expression $\phi\otimes\mathbf{v}$ is to be understood simply as $\phi\mathbf{v}$.

1.1.2 Classical Jump Conditions

Note that in deriving the local forms of balance laws (1.5) and (1.7) above, we have assumed that all the quantities were continuously differentiable inside the control volume $\omega(t)$. Whenever there exists a surface $\sigma(t)$ inside $\omega(t)$ across which a scalar or vector field ϕ is discontinuous, the continuous differentiability condition has to be relaxed and the Reynolds transport theorem has to be modified to take this discontinuity into account.

When describing surfaces inside a continuous body, we shall use two important concepts defined below.

Definition 1.1. The surface inside a body occupied by the same set of particles at each time is referred to as a *material surface*.

Definition 1.2. The surface inside a body across which a physical quantity admits a discontinuity is referred to as a *singular surface*.

The characterization of discontinuity of the physical quantity ϕ across a singular surface $\sigma(t)$ that is not necessarily material is achieved by means of its *jump* $[\![\phi]\!]$. This quantity is defined by

$$[\![\phi]\!](\mathbf{x}) := \lim_{\varepsilon \to 0^+} \left[\phi(\mathbf{x} + \varepsilon \mathbf{n}_\sigma) - \phi(\mathbf{x} - \varepsilon \mathbf{n}_\sigma)\right], \quad \forall \mathbf{x} \in \sigma(t),$$

where $\mathbf{n}_\sigma$ is the unit normal vector of $\sigma(t)$ at the point $\mathbf{x} \in \sigma(t)$. Since $\sigma(t)$ is not necessarily a closed surface, the orientation of $\mathbf{n}_\sigma$ is ambiguous a priori. In order to fix it, we need to denote the two subdomains delimited by $\sigma(t)$ and $\partial\omega(t)$ by ω_- and ω_+. The exact choice of notation is purely formal in nature, for example, if ϕ is piecewise constant, one might choose ω_- as the subdomain with the smaller value of ϕ. We then choose $\mathbf{n}_\sigma$ as the unit normal vector to $\sigma(t)$ pointing *inside* ω_+.

The modified version of the Reynolds transport theorem asserts that if ϕ is a scalar or vector defined in $\omega(t)$ that is discontinuous across $\sigma(t)$, then

$$\frac{\mathrm{d}}{\mathrm{d}t} \int_{\omega(t)\setminus\sigma(t)} \phi \,\mathrm{d}x = \int_{\omega(t)\setminus\sigma(t)} \left(\frac{\partial \phi}{\partial t} + \operatorname{div}(\phi \otimes \mathbf{v}) \right) \mathrm{d}x - \int_{\sigma(t)} [\![(\phi \otimes (\mathbf{v} - \mathbf{w}))\mathbf{n}_\sigma]\!] \,\mathrm{d}s, \tag{1.8}$$

where $\mathbf{n}_\sigma$ is again the unit normal vector of the singular surface $\sigma(t)$ with the orientation specified above, and $\mathbf{w}$ is the Eulerian velocity of $\sigma(t)$. We refer the reader to Appendix A for the proof of this theorem. It relies on a modification of the Gauss integration formulae on a domain with a singular surface that read

$$\int_{\omega(t)\setminus\sigma(t)} \operatorname{div} \mathbf{u} \,\mathrm{d}x = \int_{\partial\omega(t)} \mathbf{u} \cdot \mathbf{n}_\omega \,\mathrm{d}s - \int_{\sigma(t)} [\![\mathbf{u} \cdot \mathbf{n}_\sigma]\!] \,\mathrm{d}s, \tag{1.9}$$

$$\int_{\omega(t)\setminus\sigma(t)} \operatorname{div} \mathbb{A} \,\mathrm{d}x = \int_{\partial\omega(t)} \mathbb{A}\mathbf{n}_\omega \,\mathrm{d}s - \int_{\sigma(t)} [\![\mathbb{A}\mathbf{n}_\sigma]\!] \,\mathrm{d}s \tag{1.10}$$

for vector and tensor fields respectively. Here $\mathbf{n}_\omega$ is the unit outward normal vector to the boundary of $\omega(t)$.

Suppose that all the fields appearing in the statements of the mass and momentum balance laws are discontinuous across the non-material surface $\sigma(t) \subset \omega(t)$, and are continuously differentiable in $\omega(t) \setminus \sigma(t)$. Taking into account

the modified Reynolds transport theorem (1.8) as well as the modified Gauss integration formula (1.10), the global forms of the mass and momentum balance laws become

$$\int_{\omega(t)\setminus\sigma(t)} \left(\frac{\partial \rho}{\partial t} + \operatorname{div}(\rho \mathbf{v}) \right) \mathrm{d}x + \int_{\sigma(t)} [\![\rho(\mathbf{v} - \mathbf{w}) \cdot \mathbf{n}_\sigma]\!] \, \mathrm{d}s = 0,$$

$$\int_{\omega(t)\setminus\sigma(t)} \left(\frac{\partial}{\partial t}(\rho \mathbf{v}) + \operatorname{div}(\rho \mathbf{v} \otimes \mathbf{v}) \right) \mathrm{d}x + \int_{\sigma(t)} [\![(\rho \mathbf{v} \otimes (\mathbf{v} - \mathbf{w})) \mathbf{n}_\sigma]\!] \, \mathrm{d}s = \\ = \int_{\omega(t)\setminus\sigma(t)} (\rho \mathbf{b} + \operatorname{div} \mathbb{T}) \, \mathrm{d}x + \int_{\sigma(t)} [\![\mathbb{T} \mathbf{n}_\sigma]\!] \, \mathrm{d}s,$$

respectively.

Applying the localization lemma now yields not only the local balance equations in $\omega(t) \setminus \sigma(t)$, but also jump conditions on $\sigma(t)$

$$[\![\rho(\mathbf{v} - \mathbf{w}) \cdot \mathbf{n}_\sigma]\!] = 0, \tag{1.11}$$

$$[\![(\rho \mathbf{v} \otimes (\mathbf{v} - \mathbf{w})) \mathbf{n}_\sigma - \mathbb{T} \mathbf{n}_\sigma]\!] = \mathbf{o}. \tag{1.12}$$

The former imposes the *continuity of mass flux* across $\sigma(t)$ and the latter relates the *jump in traction* $\mathbb{T}\mathbf{n}_\sigma$ to the *jump of momentum flux* across $\sigma(t)$.

The primary motivation behind the topic of this thesis is a paper by Chambat et al. [2014], where the classical form (1.12) of the momentum jump condition is contested for a specific flow discussed in more detail in one of the following sections.

Although the fundamental idea behind the continuous description of matter is the continuity of quantities of physical interest, the admission of singular surfaces into models is valid, especially for systems with regions occupied by substances whose properties differ considerably. The most prevalent example of this are *phase interfaces*. There are many examples of physical systems with multiple phases of one material represented, glaciers or the Earth's inner core to name a few. Indeed, the jump conditions discussed in this thesis are used for example by Corrieu et al. [1995] to model mantle flow evolution and compare it to the present-day state of the Earth.

Another example of a problem describing a phase change in a dynamic medium is the thermo-mechanically coupled *Stefan problem*. It models a system with a phase interface that can move in time. Besides its appeal to the theory of PDE, it can be used in geophysics to model lava flow after an eruption as shown by Lister [1994] or solidification of a liquid in a channel, as demonstrated by Myers and Low [2011].

1.2 Description of Phase Interfaces

[Slattery et al., 2007, p. 7] define the *phase interface* as the "region separating two phases in which properties of the material differ from those of the adjoining phases". The experimental hints of the specific behavior of a system near an interface have been established by Defay et al. [1966]. From a purely physical point of view, the properties of a system in the neighborhood of a phase interface are best described by molecular modelling and statistical mechanics. While the molecular description of interfaces is very realistic and leads to sensible predictions

of system behavior on a macroscopic scale, the continuous approach is of equal importance due to relative ease of solution of problems and direct relation to the analysis of experimental data. In continuum mechanics, there are two available models of phase interfaces: the *three-dimensional region* and the *two-dimensional surface*.

1.2.1 Phase Interface as a Three-Dimensional Interfacial Region

The obvious first choice of phase interface description in continuum mechanics is to treat it as a region of finite thickness. As [Slattery et al., 2007, p. 8] mention, there exists a theory describing the relationships between stress and deformation for this view of a phase interface, but it essentially assumes a static system and therefore yields no results as far as dynamic properties of interfaces are concerned.

For the purposes of this thesis, we shall adopt a *diffuse interface approach* used by Chambat et al. [2014], where the physical quantities such as density, velocity, or viscosity are supposed to undergo a rapid but smooth change inside a *transitional layer* of finite thickness. We then assume that the governing equations formulated for each of the *homogeneous phases*[2] also hold inside the interfacial region.

1.2.2 Phase Interface as a Dividing Surface

It is clear from the previous section that while the three-dimensional model is still quite realistic in its description of material properties inside the interface, it is quite difficult to use in general applications. As an alternative, Slattery et al. [2007] introduce the concept of a *dividing surface*, which is a hypothetical two-dimensional region lying within or near the two homogeneous phases. The accumulated effects of the interface on the adjoining phases are accounted for by *excess surface densities* and *fluxes* of physical quantities.

The simplest nontrivial example of a physical quantity defined on a dividing surface is the *isotropic surface tension*. It arises from interpreting the excess forces acting between the interface and the neighboring phases as the *surface Cauchy stress tensor* $\mathbb{T}_\sigma$. If we assume that the interface behaves like an isotropic membrane, then the surface Cauchy stress tensor can be prescribed as $\mathbb{T}_\sigma = s\mathbb{I}_\sigma$, s being the scalar surface tension and $\mathbb{I}_\sigma$ denoting the identity tensor on the surface $\sigma(t)$ defined by

$$\mathbb{I}_\sigma := \mathbb{I} - \mathbf{n}_\sigma \otimes \mathbf{n}_\sigma.$$

Instead of the simple jump condition (1.12), the momentum balance equation on such a surface reads (cf. Slattery et al. [2007])

$$[\![\mathbb{T}\mathbf{n}_\sigma - (\rho\mathbf{v} \otimes (\mathbf{v} - \mathbf{w}))\mathbf{n}_\sigma]\!] = \operatorname{div}_\sigma \mathbb{T}_\sigma,$$

where $\operatorname{div}_\sigma$ is the surface divergence operator. The right-hand side of the above expression can be rewritten as

$$\operatorname{div}_\sigma (s\mathbb{I}_\sigma) = \nabla_\sigma s - s \operatorname{div}_\sigma \mathbb{I}_\sigma = \nabla_\sigma s - 2\kappa\mathbf{n}_\sigma, \tag{1.13}$$

[2] [Slattery et al., 2007, p. 8] define a homogeneous phase as a subdomain where all constitutive relations hold uniformly.

where ∇_σ is the surface gradient and κ denotes the mean curvature of the surface. The physical interpretation of the first term is the *Marangoni effect* relating the traction along the phase interface to the gradient of surface tension, and the second term corresponds to the *Young-Laplace law*.

Besides being simple and illustrative, the above example is pertinent to the main topic of this thesis. The alternative stress tensor jump condition proposed by Chambat et al. [2014] takes a form analogous to (1.13), which motivates Chambat et al. [2014] to attribute the jump in stress to some kind of *dynamic* surface tension.

1.3 Quasi-Static Stokes Flow

Even for very simple fluid models, the solution of equations (1.5) and (1.7) in their general form is extremely complicated or not feasible. It is therefore commonplace to simplify the equations by neglecting certain terms according to physical scaling arguments.

For the purposes of this thesis, we have chosen to treat the *quasi-static Stokes flow problem*, as introduced, e.g., by [Sangtae and Seppo, 1991, p. 9 – 10]. In this type of flow, also called *steady creeping flow*, the partial derivatives with respect to time are neglected, as well as the nonlinear inertia term $\rho\mathbf{v}\otimes\mathbf{v}$ in the momentum balance and the corresponding jump condition (1.12). Furthermore, the absence of body forces is assumed, translating to $\mathbf{b}=\mathbf{o}$. The resulting set of governing equations and jump conditions reads

$$\operatorname{div}(\rho\mathbf{v}) = 0, \qquad \text{in } \omega(t)\setminus\sigma(t), \tag{1.14}$$

$$\operatorname{div}\mathbb{T} = \mathbf{o}, \qquad \text{in } \omega(t)\setminus\sigma(t), \tag{1.15}$$

$$[\![\rho\mathbf{v}\cdot\mathbf{n}_\sigma]\!] = 0, \qquad \text{on } \sigma(t), \tag{1.16}$$

$$[\![\mathbb{T}\mathbf{n}_\sigma]\!] = \mathbf{o}, \qquad \text{on } \sigma(t). \tag{1.17}$$

In both jump conditions (1.16) and (1.17) we also assume that the singular surface $\sigma(t)$ is *static*, i.e., $\mathbf{w}\equiv\mathbf{o}$, for the sake of simplicity.

Although the simplified equations above are very convenient from a mathematical point of view, their interpretation in the physical context is not trivial.

First, the terms involving partial derivatives with respect to time as well as the convective derivative of velocity in the momentum balance (1.7) are omitted. This can be justified by an *a priori* assumption of the explicit time-independence of physical quantities and by deriving the dimensionless form of the momentum balance equation in a way that introduces the *Reynolds number*. The Reynolds number compares the characteristic lengths and velocities of the system, and for very small lengths or very slow speeds we can justify working with the limiting case of the Reynolds number equal to zero, which reduces the system to the one presented here. This is the argument made by Sangtae and Seppo [1991].

However, there is an argument, made for example by [Matyska, 2005, p. 31], that is more complete from a physical point of view. It takes into account the full thermodynamically coupled system and introduces a dimensionless form of the momentum balance equation involving the *Prandtl number* that compares the kinematic viscosity of the fluid with its heat transfer properties. Then, if the physical properties of the studied system are such that the limit as the Prandtl

number goes to infinity is relevant, both the local and convective time derivatives in the momentum balance can be neglected.

Another point concerns the inclusion of ρ inside the divergence operator in Equation (1.14). In the sharp interface approach, we assume the density to be constant on each side of the dividing surface, both phases of the fluid being incompressible. On the other hand, if we solve the system with a diffuse interface, the density is assumed to change rapidly but smoothly inside the transitional layer and the governing equations are assumed valid both inside and outside the layer, making the fluid effectively compressible.

Although the difference may seem formal at first sight, the difference between compressible and incompressible flows is significant both in terms of the mathematical analysis and the underlying physical interpretation. The physical argument that leads to a mass balance in the form (1.14) is the so called *compressible extended Boussinesq approximation*.

For compressible fluids, density ρ, pressure p, and temperature θ of the system are related via the *equation of state* $\rho = \rho(p, \theta)$ that is postulated as one of the constitutive relations. As formulated by [Matyska, 2005, p. 26], "the idea of the Boussinesq approximation consists in the linearization of the basic laws of conservation near a reference hydrostatic state", i.e., the state with $\mathbf{v} \equiv \mathbf{o}$. This reference state is characterized by a density ρ_0, a pressure p_0, and a temperature θ_0. The equation of state is linearized with respect to the variations of temperature $\Delta\theta := \theta - \theta_0$, effectively including the hydrostatic pressure and reference temperature dependencies in the spatial dependence of the reference density. Substituting this linearized model into the mass balance equation leads to its form (1.14) stated above. A more rigorous derivation of a problem setting where ρ is essentially independent of p based on fundamental thermodynamic assumptions was developed by Bechtel et al. [2003], but is beyond the scope of this thesis.

As we have already mentioned above, the work presented in this thesis builds on an article by Chambat et al. [2014] that puts into question the validity of the traction jump condition (1.17) usually prescribed in this type of flow model. Chambat et al. [2014] argue that the correct jump condition to be prescribed in this case is

$$[\![\mathbb{T}\mathbf{n}_\sigma]\!] = s\kappa\mathbf{n}_\sigma - \nabla_\sigma s, \tag{1.18}$$

where κ is the sum of principal curvatures of $\sigma(t)$, ∇_σ denotes the surface gradient, and s is the *dynamic surface tension* given by

$$s = -2(\rho\mathbf{v}\cdot\mathbf{n}_\sigma)\lim_{\varepsilon\to 0^+}\int_{\mathbf{x}-\varepsilon\mathbf{n}_\sigma}^{\mathbf{x}+\varepsilon\mathbf{n}_\sigma}\eta\frac{\partial}{\partial q^3}\left(\frac{1}{\rho}\right)\,\mathrm{d}q^3,$$

q^3 being the local generalized coordinate normal to the surface $\sigma(t)$.

It is evident that the form of the jump resembles that of the interface momentum balance in presence of surface tension from Equation (1.13)[3], hence the name and the notation for s. However, as we shall see in the next chapter, the derived jump

[3]The only difference between Equations (1.13) and (1.18) is in the sign. This is due to the convention used in the definition of surface tension. The surface tension model interprets s as an *extension*, which motivates the definition $\mathbb{T}_\sigma = s\mathbb{I}_\sigma$. As an example of the alternative convention, the pressure in the hydrostatic model is interpreted as a *compression* and the Cauchy stress tensor then reads $\mathbb{T} = -p\mathbb{I}$.

condition is not an intrinsic property of the surface, but arises from the dynamic properties of the studied system.

Besides having a relatively simple structure, the steady Stokes flow problem has numerous physical applications. It can be used to model flows of viscous fluids at very slow speeds or in systems with very small characteristic lengths. One of prominent examples of its practical use is the study of mantle dynamics in geophysics by Corrieu et al. [1995] among others.

As for the fluid rheology, the starting point for all discussions that follow is the *linear viscous* (or Newtonian) *fluid*. Its Cauchy stress tensor is given by

$$\mathbb{T} = -p\mathbb{I} + \eta \left[\nabla \mathbf{v} + (\nabla \mathbf{v})^T\right] + \lambda(\operatorname{div} \mathbf{v})\mathbb{I}, \tag{1.19}$$

where p denotes pressure, $\mathbf{v}$ is the Eulerian velocity field, $\mathbb{I}$ is the identity tensor, and λ and η are bulk and shear viscosities, respectively.

Chapter Summary The work presented in this thesis deals with modelling of fluid flow on domains with interfaces. This chapter has introduced the fundamental concepts of continuum mechanics which will be further elaborated in the subsequent chapters of the thesis. We have namely given a review of the various theoretical descriptions of interfaces and a review of their mathematical treatment has been given in the form of the modified Reynolds transport theorem and the discussion of isotropic surface tension. Finally, we have set up the problem that is the basis of the investigations that follow, discussing the physical significance of the chosen flow regime as well as the various prescriptions for the traction jump condition that will be compared later on.

Chapter 2

Dynamic Surface Tension – Motivation

The main reason behind the introduction of dynamic surface tension into the description of flows across an interface is the inconsistency between the theoretically postulated behavior of a continuous system with a singular surface and the results of numerical experiments. This chapter aims at demonstrating this inconsistency on a model of *two-dimensional planar flow* in the stationary Stokes regime discussed above. The particular structure of this model allows its fully analytic resolution in the *sharp interface* approach as well as numerical solution in the *diffuse interface* approach. By comparing the exact solution for a sharp interface and continuous traction with a numerical solution for a diffuse interface we show that the two differ considerably, and that the inconsistency in the two approaches can be overcome by introducing a nontrivial traction jump corresponding to *dynamic surface tension*.

Besides motivating the work presented in the subsequent chapters, these results reproduce the results published by Chambat et al. [2014], shown in Figure 1, using different methods.

2.1 Problem Setting

Consider the two-dimensional domain

$$\Omega := \left(-\frac{\pi}{k}, \frac{\pi}{k}\right) \times (-h, h) \ni (x, z)$$

with $k, h > 0$ given. We are interested in the quasi-static Stokes flow inside this domain, i.e., we let the governing equations (1.14), (1.15) hold in Ω.

To ensure that the problem is well-posed, boundary conditions need to be specified on $\partial\Omega$. Motivated by Chambat et al. [2014], we prescribe the mass flow at the horizontal parts of the boundary and a free slip condition at the vertical parts of the boundary. The full set of boundary conditions then reads

$$(\rho\mathbf{v} \cdot \mathbf{n})(z = \pm h) = \Psi_0 \cos(kx), \tag{2.1}$$

$$(\mathbf{v} \cdot \mathbf{n})\left(x = \pm\frac{\pi}{k}\right) = 0, \quad (\mathbf{t} \cdot \mathbb{T}\mathbf{n})\left(x = \pm\frac{\pi}{k}\right) = 0. \tag{2.2}$$

If we decide to treat the interface as a singular surface

$$\Sigma := \{(x, z) \in \Omega;\ z = 0\},$$

then we are essentially solving the two governing equations (1.14) and (1.15) on the subdomains

$$\Omega_1 := \left(-\frac{\pi}{k}, \frac{\pi}{k}\right) \times (-h, 0), \quad \Omega_2 := \left(-\frac{\pi}{k}, \frac{\pi}{k}\right) \times (0, h),$$

and we need to prescribe jump conditions at the interface. This setting is shown schematically in Figure 2.1a.

Taking into account the mass flux jump condition (1.16) and the fact that $\mathbf{n}_\Sigma = \mathbf{e}_z$ is the normal vector of the dividing surface Σ, the first jump condition reads

$$(\rho v_z)(z = 0^+) = (\rho v_z)(z = 0^-). \tag{2.3}$$

For the traction jump, our goal is to compare the classical jump condition (1.17) to the condition (1.18) suggested by Chambat et al. [2014]. To account for both of these conditions in the formal manipulations, we prescribe the traction jump as

$$T_{xz}(z = 0^+) - T_{xz}(z = 0^-) = J \sin(kx), \tag{2.4}$$

where $J = 0$ for the classical jump condition and $J = 2\eta[\![1/\rho]\!]\rho\mathbf{v} \cdot \mathbf{n}$ for the Chambat et al. [2014] jump condition assuming continuous rheology ($[\![\eta]\!] = 0$).

Instead of considering the interface as the sharp singular surface Σ, we can treat it as a *transitional layer* of very small nontrivial thickness proportional to some $\varepsilon > 0$ defined by

$$\widetilde{\Sigma} := \left(-\frac{\pi}{k}, \frac{\pi}{k}\right) \times (-\alpha\varepsilon, \alpha\varepsilon).$$

The exact value of the proportionality constant α is of little importance here, although it will be discussed in more detail in one of the subsequent chapters. For now, it is sufficient to assume that ε is a small parameter and that the governing equations (1.14), (1.15) hold inside $\widetilde{\Sigma}$. The illustration of this setting is in Figure 2.1b.

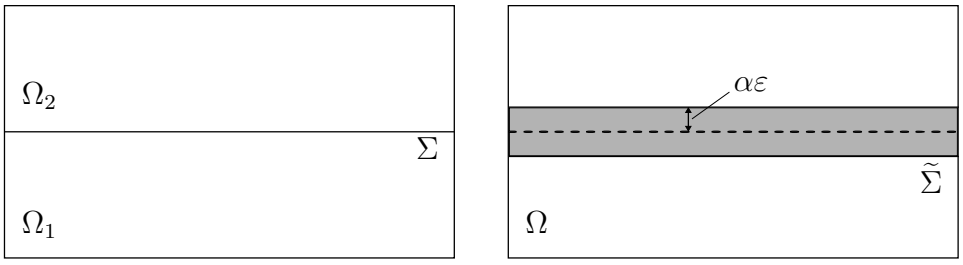

(a) sharp interface **(b)** diffuse interface

Figure 2.1: Sketches of the two interface models considered in this chapter. For the full analytical resolution, we assume that the governing equations hold in two subdomains Ω_1, Ω_2 with a possible discontinuity in the solution across a sharp interface Σ. For the numerical experiment, we solve the governing equations in the entire domain Ω, and we assume that the discontinuities in physical quantities are regularized across a transitional layer $\widetilde{\Sigma}$.

2.2 Exact Solution for the Sharp Interface

Let us proceed to finding the exact solution of the governing equations in the sharp interface case. The solution procedure presented here is similar to the one published by Chambat et al. [2014]. If we choose $\Psi(x, z)$ such that

$$\rho v_x = -\frac{\partial \Psi}{\partial z}, \quad \rho v_z = \frac{\partial \Psi}{\partial x} \qquad \text{in } \Omega_i,\ i = 1, 2,$$

then the mass balance equation (1.14) is satisfied trivially provided that Ψ is sufficiently smooth.

Remark. The function Ψ is a hydrodynamic auxiliary quantity referred to as the *stream function*.

If we then take the curl of the momentum balance equation (1.15), substitute for $\mathbb{T}$ from the linear rheology assumption (1.19), and introduce the stream function Ψ, we get

$$\Delta \left(\operatorname{div} \left(\frac{1}{\rho} \nabla \Psi \right) \right) = 0 \quad \text{in } \Omega_1, \Omega_2.$$

For simplicity, assume $\rho = \rho_i = \text{const.}$ in each of the subdomains Ω_1, Ω_2. The above equation thus reduces to the biharmonic equation for the stream function

$$\Delta^2 \Psi = 0 \quad \text{in } \Omega_1, \Omega_2. \tag{2.5}$$

We look for a solution of the form

$$\Psi(x, z) = \hat{\Psi}(z) \sin(kx) \quad \text{in } \Omega_1, \Omega_2.$$

Equation (2.5) is therefore further simplified to the fourth order ODE

$$\hat{\Psi}^{(4)} - 2k^2 \hat{\Psi}^{(2)} + k^4 \hat{\Psi} = 0 \tag{2.6}$$

for $\hat{\Psi}(z)$ on the two subdomains Ω_1, Ω_2. Its general solution reads

$$\hat{\Psi}(z) = (A_i + B_i z)\mathrm{e}^{-kz} + (C_i + D_i z)\mathrm{e}^{kz}, \quad z \in \Omega_i,\ i = 1, 2, \tag{2.7}$$

where A_i, B_i, C_i, D_i, $i = 1, 2$ are constants. To fix these constants, we have to incorporate the boundary and jump conditions introduced above. The mass flux boundary condition (2.1) translates to

$$\hat{\Psi}(\pm h) = \frac{\Psi_0}{k}, \quad \hat{\Psi}'(\pm h) = 0 \tag{2.8}$$

when interpreted using the stream function. Due to the assumed form of the solution, the free slip boundary conditions (2.2) at $x = \pm\pi/k$ are satisfied automatically. The mass flux jump condition (1.16) and the traction jump condition (1.17) expressed in terms of $\hat{\Psi}$ read

$$\hat{\Psi}(0^+) = \hat{\Psi}(0^-), \tag{2.9}$$

$$\begin{cases} \left(\dfrac{\hat{\Psi}''(0^+)}{\rho_2} - \dfrac{\hat{\Psi}''(0^-)}{\rho_1} \right) + k^2 \left(\dfrac{\hat{\Psi}(0^+)}{\rho_2} - \dfrac{\hat{\Psi}(0^-)}{\rho_1} \right) = 0 & \text{in classical case,} \\ \left(\dfrac{\hat{\Psi}''(0^+)}{\rho_2} - \dfrac{\hat{\Psi}''(0^-)}{\rho_1} \right) - k^2 \left(\dfrac{\hat{\Psi}(0^+)}{\rho_2} - \dfrac{\hat{\Psi}(0^-)}{\rho_1} \right) = 0 & \text{in Chambat case,} \end{cases} \tag{2.10}$$

respectively. Two more jump conditions need to be added for the system to be uniquely solvable. The first is the *kinematic condition* $[\![v_x]\!] = 0$ that translates to

$$\frac{\hat{\Psi}'(0^+)}{\rho_2} = \frac{\hat{\Psi}'(0^-)}{\rho_1}. \tag{2.11}$$

The second is obtained by differentiating the continuity condition for the zz-component of the Cauchy stress tensor $[\![T_{zz}]\!] = 0$ with respect to x and introducing the stream function. After some manipulation, we get the condition

$$\frac{\hat{\Psi}'''(0^+)}{\rho_2} = \frac{\hat{\Psi}'''(0^-)}{\rho_1}. \tag{2.12}$$

Conditions (2.8) – (2.12) for $\hat{\Psi}$ in the form (2.7) present in total a system of 8 linear equations for 8 unknowns A_i, B_i, C_i, D_i, $i = 1, 2$. We used the *Wolfram Mathematica* software to solve this system symbolically, and we have plotted the resulting velocity fields for both the classical and the Chambat et al. [2014] traction jump conditions. The plots can be found in Figures 2.3a and 2.3b. We shall now proceed to the numerical solution of the diffuse interface model before discussing the results of the analytical resolution of the sharp interface model above. The exact choice of physical parameters such as densities on the subdomains or the value of viscosity will be addressed as part of the implementation of the numerical experiment.

2.3 Numerical Solution for the Diffuse Interface

2.3.1 Finite Element Method

In almost every physical theory, the formulation of fundamental principles results in one or more PDEs involving quantities changing in time and space. However, in many settings among which countless examples from continuum mechanics, the physical fields or the computational domains are not regular enough to enable classical PDE description. The modern theory of PDEs therefore introduces the concept of a *weak derivative* and the *weak formulation* of a PDE problem, which relax the regularity conditions on the quantities involved. Although the full exposition of this mathematical theory is far beyond the scope of this thesis, we note that one of the motivation for weakly formulated PDEs are integral forms of physical laws such as those mentioned in Section 1.1.

For practical purposes, physical PDE systems can be solved almost exclusively (except for a few special cases) via numerical methods. The *finite element method* is possibly the most widespread method of approximating the weak solution of a PDE introduced, e.g., in the book by Ciarlet [2002]. In the case of linear equation, the method interprets the weak formulation of a PDE as an abstract variational problem of the form

$$\text{Find } u \in U: \quad a(u, v) = l(v) \quad \forall v \in V,$$

where U is the solution space, v is called a *test function*, V is the test function space, a is a bilinear form, and l is a linear form. Provided that the forms a and l

satisfy certain conditions, it can be proved that the above variational problem has a unique solution.

The main idea of the finite element method is to define a mesh on the computational domain and approximate the spaces U, V by finite-dimensional spaces U_h, V_h (called *finite element spaces*) defined on the mesh (for example spaces of piecewise polynomials). If the spaces U_h, V_h have the correct approximation properties, then the *discrete solution* u_h of the *discrete problem*

$$\text{Find } u_h \in U_h : \quad a(u_h, v_h) = l(v_h) \quad \forall v_h \in V_h$$

converges in some sense to the exact solution u. The approximation properties of finite element spaces rely on the interpolation theory in Sobolev spaces and will not be treated in detail here, although when discussing specific PDE problem implementation, relevant literature references will be given.

In this section, we discuss numerical implementation of the diffuse interface model described in Section 2.1. For illustrative purposes, we fix $h = 1$, $k = \frac{\pi}{5}$, which then translates to $\Omega = (-5, 5) \times (-1, 1)$.

2.3.2 Formulation and Implementation

If we interpret the interface at $z = 0$ as a transitional layer, then the density is assumed to be continuously differentiable in the whole domain Ω, but varies rapidly from ρ_1 to ρ_2. The density transitional profile we shall use in the implementation is taken directly from Chambat et al. [2014] and reads

$$\rho(z) = \rho_1 + \frac{\rho_2 - \rho_1}{2}\left[1 + \tanh\left(\frac{z}{\varepsilon}\right)\right],$$

where ε is a small parameter. For the linear constitutive relation given by (1.19), the system of equations to be solved is

$$\operatorname{div}(\rho\mathbf{v}) = 0, \quad \operatorname{div}\left[-p\mathbb{I} + 2\eta\mathbb{D}(\mathbf{v}) + \lambda(\operatorname{div}\mathbf{v})\mathbb{I}\right] = \mathbf{o} \qquad \text{in } \Omega, \tag{2.13}$$

where we have introduced the notation

$$\mathbb{D}(\mathbf{v}) := \frac{1}{2}\left[\nabla\mathbf{v} + (\nabla\mathbf{v})^T\right]$$

for the symmetric part of a gradient. The boundary conditions for velocity are given by (2.1) and (2.2). Since the structure of the momentum balance equation implies that the pressure is determined up to a constant, it is natural to fix a point value of pressure. Hence, the pressure "boundary" condition we impose is

$$p(x = -5, z = 1) = 0. \tag{2.14}$$

In order to be able to apply the existing mathematical theory, we have to further transform the system (2.13). Set $\mathbf{u} := \rho\mathbf{v}$. Rewriting Equations (2.13) in terms of $\mathbf{u}$ yields

$$\operatorname{div}\mathbf{u} = 0 \qquad \text{in } \Omega, \tag{2.15a}$$

$$\operatorname{div}\left\{-p\mathbb{I} + 2\eta\mathbb{D}\left(\frac{\mathbf{u}}{\rho}\right) + \lambda\left[\operatorname{div}\left(\frac{\mathbf{u}}{\rho}\right)\right]\mathbb{I}\right\} = \mathbf{o} \qquad \text{in } \Omega. \tag{2.15b}$$

The boundary conditions for $\mathbf{u}$ derived from boundary conditions (2.1), (2.2) are

$$u_x(x = \pm 5) = 0, \quad \mathbf{u}(z = \pm h) = \Psi_0 \cos\left(\frac{\pi}{5}x\right)\mathbf{e}_z. \tag{2.16}$$

While from a physical point of view we have formulated the governing equations in terms of momentum instead of velocity, from a mathematical point of view the system (2.15) can be interpreted as a mixed problem for $\mathbf{u}$ reminiscent of the *incompressible* Stokes problem, which enables relatively straightforward implementation.

Following the procedure outlined, e.g., by [Larson and Bengzon, 2013, p. 292 – 295], we define the following test function spaces:

$$V := \left\{\mathbf{w} \in \left[H^1(\Omega)\right]^2;\ \mathbf{w}|_{\partial\Omega} = \mathbf{o}\right\},$$
$$Q := \left\{q \in L^2(\Omega);\ q(x = -5, z = 1) = 0\right\}.$$

Here, $L^2(\Omega)$ is the space of Lebesgue square-integrable functions on Ω and $H^1(\Omega)$ denotes the Sobolev space of L^2-integrable functions with L^2-integrable first weak derivatives. The solution space for pressure p is identical to the corresponding test function space Q, whereas the momentum solution space has to take the boundary conditions into account. Hence, we define

$$U := \left\{\mathbf{u} \in \left[H^1(\Omega)\right]^2;\ u_x(x = \pm 5) = 0,\ \mathbf{u}(z = \pm h) = \Psi_0 \cos\left(\frac{\pi}{5}x\right)\mathbf{e}_z\right\}.$$

To derive the weak formulation of the problem, we multiply Equation (2.15a) by $q \in Q$, take the inner product of Equation (2.15b) with $\mathbf{w} \in V$, and integrate both equations over the domain Ω. After integrating the terms involving first derivatives of pressure and second derivatives of momentum by parts and acknowledging that thanks to the definition of V the boundary integrals vanish, we get

$$\int_\Omega q \operatorname{div}\mathbf{u}\,\mathrm{d}x = 0, \quad q \in Q, \tag{2.17}$$

$$\begin{aligned}\int_\Omega p \operatorname{div}\mathbf{w}\,\mathrm{d}x - 2\int_\Omega \eta\mathbb{D}\left(\frac{\mathbf{u}}{\rho}\right) : \mathbb{D}(\mathbf{w})\,\mathrm{d}x - \\ - \int_\Omega \lambda \operatorname{div}\left(\frac{\mathbf{u}}{\rho}\right)\operatorname{div}\mathbf{w}\,\mathrm{d}x = 0, \quad \mathbf{w} \in V,\end{aligned} \tag{2.18}$$

where : denotes the tensor inner product. Finally, summing these two equations gives us the abstract variational problem

$$\text{Find } (\mathbf{u}, p) \in U \times Q: \quad a\left[(\mathbf{u}, p), (\mathbf{w}, q)\right] = 0 \quad \forall q \in Q,\ \forall \mathbf{w} \in V \tag{2.19}$$

with

$$\begin{aligned}a\left[(\mathbf{u}, p), (\mathbf{w}, q)\right] = \int_\Omega q \operatorname{div}\mathbf{u}\,\mathrm{d}x + \int_\Omega p \operatorname{div}\mathbf{w}\,\mathrm{d}x - \\ - 2\int_\Omega \eta\mathbb{D}\left(\frac{\mathbf{u}}{\rho}\right) : \mathbb{D}(\mathbf{w})\,\mathrm{d}x - \int_\Omega \lambda \operatorname{div}\left(\frac{\mathbf{u}}{\rho}\right)\operatorname{div}\mathbf{w}\,\mathrm{d}x.\end{aligned}$$

Remark. Problem (2.19) is a special case of the so-called *mixed problem*, where multiple variables from different spaces are solved for. As [Larson and Bengzon, 2013, p. 295] show, this problem can be viewed as a constrained minimization problem, where the functional that is minimized is derived from (2.18) and the "incompressibility" condition (2.17) acts as a constraint. This leads to the mathematical interpretation of pressure in incompressible Stokes flows as a *Lagrange multiplier* corresponding to the *incompressibility condition*.

We can now proceed to defining the appropriate finite element spaces U_h, V_h, Q_h. In order for the numerical approximation $(\mathbf{u}_h, p_h)$ to converge to the exact solution $(\mathbf{u}, p)$ of Problem (2.19), the spaces V_h and Q_h have to satisfy the *Babuška-Brezzi condition*

$$\inf_{q_h \in Q_h} \sup_{\mathbf{w}_h \in V_h} \frac{\int_\Omega q_h \operatorname{div} \mathbf{w}_h \, \mathrm{d}x}{\|q_h\|_{0,\Omega} \, \|\mathbf{w}_h\|_{1,\Omega}} \geq \beta \tag{2.20}$$

for some $\beta > 0$ independent of h, as is proved, e.g., by [Ern and Guermond, 2004, Proposition 4.13]. The symbols $\|\cdot\|_{0,\Omega}$ and $\|\cdot\|_{1,\Omega}$ denote the norms in the spaces $L^2(\Omega)$ and $H^1(\Omega)$ respectively.

We solve the above-mentioned variational problem on a mesh consisting of triangles. Its outline can be seen in Figure 2.2. Note that the mesh is much finer around the interface $z = 0$. This is motivated by the expected behavior of the interpolated functions. We expect the changes in z of all the relevant quantities to be much more significant in the vicinity of $z = 0$ compared to the two subdomains $z \ll 0$ and $z \gg 0$. In most of the usually encountered settings, finite element spaces consist of functions that belong to a certain space of polynomials on each triangle of the mesh and satisfy relevant *continuity conditions* to ensure the required regularity of interpolated functions.

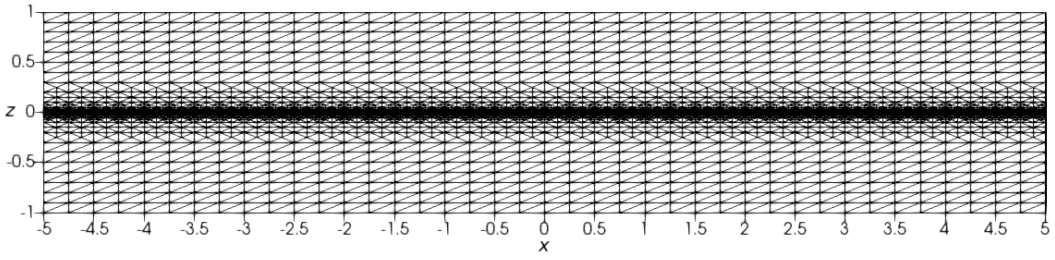

Figure 2.2: The mesh used in the diffuse interface version of the finite element solution of the planar Stokes flow problem. Close to the interface $z = 0$, the mesh has been refined multiple times to achieve greater precision in approximated functions in the region where their variations are expected to be comparatively large. Note that all plotted quantities are considered non-dimensional and without explicit physical units.

The next step is therefore to choose the spaces of polynomials for V_h and Q_h pertinent to our problem. As [Ern and Guermond, 2004, p. 186 – 189] show, not every combination works. Problem (2.19) has a *saddle point structure*, which makes it numerically unstable, and many choices of polynomial space combination lead to unwanted oscillatory components called *spurious modes* appearing in the numerical solution due to the violation of the Babuška-Brezzi condition (2.20). The standard choice of finite element spaces that satisfy the condition (2.20) is

based on the so-called *Taylor-Hood element*, where the restrictions of functions from V_h to each element (triangle in our case) are polynomials of degree $k+1$ and the restrictions of functions from Q_h to each element are polynomials of degree k, for some $k \in \mathbb{N}$. The approximation U_h of the solution space is constructed similarly to V_h, the only difference being in the conditions on the behavior of the functions on $\partial\Omega$. For the purposes of our numerical experiments, we have chosen the Taylor-Hood mixed element with $k = 1$.

Following the results published by Chambat et al. [2014], we fix the values of parameters[1] of the implementation as

$$\rho_1 = 1, \quad \rho_2 = 2, \quad \eta = 1, \quad \lambda = 1000, \quad \Psi_0 = 1, \quad \varepsilon = 0.003.$$

Note that since there is no mention of the exact value of λ in the article by Chambat et al. [2014], we have set it to a value large enough to capture the "almost incompressible" nature of the problem setting. We have also decreased the value of ε from the article value 0.03 to emphasize that the diffuse interface approach is to be interpreted as a limiting process here.

Remark. While the exact values of physical parameters were not needed for the sharp interface calculations in Section 2.2, the values above were chosen for the plots shown in Figures 2.3a and 2.3b.

The *FEniCS* software environment was used for practical implementation of the method described above. The FEniCS project is a collaborative software package aimed at creating "easy, intuitive, efficient, and flexible software for solving partial differential equations [...] using finite element methods" (taken from the FEniCS tutorial book by [Langtangen and Logg, 2017, p. 3]). Its detailed presentation can be found in Alnaes et al. [2015].

2.4 Results and Interpretation

The resulting velocity component fields computed in the numerical experiment are in Figure 2.3c, along with the exact solutions of the sharp interface model from above. The exact solution plots were generated using Wolfram Mathematica and the solution of the finite element numerical experiment was plotted in *ParaView* (cf. Ahrens et al. [2005]).

If we compare the fields obtained numerically with those computed analytically before, we see that while the z-components of the velocity fields are virtually identical in all three cases, the classical traction jump in the sharp interface approach leads to an x-component of $\mathbf{v}$ that differs considerably from the diffuse interface numerical approximation. On the other hand, the traction jump proposed by Chambat et al. [2014] corresponds very well to the fields computed in this numerical experiment.

Besides serving as a proof of reproducibility for the results presented by

[1] Since the interest of the numerical experiment is primarily mathematical, we omit the units of these parameters. This might also be interpreted as a consequence of the scaling procedure from Section 1.3, since now we are effectively working with dimensionless variables. Nevertheless, in Chapter 5 the issue of exact values of these parameters for a real physical system is addressed.

Chambat et al. [2014][2], the results presented in this section serve as evidence for the Chambat et al. [2014] traction jump condition as the correct sharp interface limit with respect to the diffuse interface approach. It is also a motivation for further study of implications of solving the governing equations "inside" the interface presented in the chapters that follow.

2.5 Note on Finite Element Implementation of the Sharp Interface Model

We restricted ourselves to the diffuse interface point of view in the numerical experiment to illustrate the usual approach to this sort of problem. Taking the diffuse interface as an approximation of a system whose theoretical description involves a sharp interface is very convenient. The main difficulty of implementing the sharp interface case lies in the discontinuous nature of the quantities in the equations. This restricts the possible choice of elements leading to stable numerical schemes considerably. Furthermore, the implementation is made even more challenging by the fact that the variational problem has to contain information of the exact form of the discontinuity in the solution at the interface, given by the prescribed traction jump. While transcending the scope of the work presented here, these difficulties can nevertheless be overcome and a more detailed investigation of this problem setting is a subject of ongoing research.

Chapter Summary The aim of this chapter was to illustrate the pitfalls of taking the diffuse interface approach with all governing equations valid inside the interface as an approximation of the sharp interface model with continuous traction on a simple model of two-dimensional planar Stokes flow. For the sharp interface model, we found and compared exact forms of velocity fields for the trivial traction jump as well as the Chambat et al. [2014] traction jump involving dynamic surface tension. We then formulated the diffuse interface model in terms of the finite element method and compared the solution to the sharp interface exact solutions, coming to the conclusion that the appropriate sharp interface limit with respect to the diffuse interface approach is the one involving dynamic surface tension in this particular simple case. This leads to further investigations of the limit behavior of the diffuse interface solutions and its interpretation in what follows.

[2]The method Chambat et al. [2014] used differs from the method presented in this work in that Chambat et al. [2014] solved the ODEs obtained via the stream function method numerically using Runge-Kutta methods in all three cases, whereas the solution we have presented for the sharp interface model is fully analytical, and the diffuse interface model is implemented in finite elements.

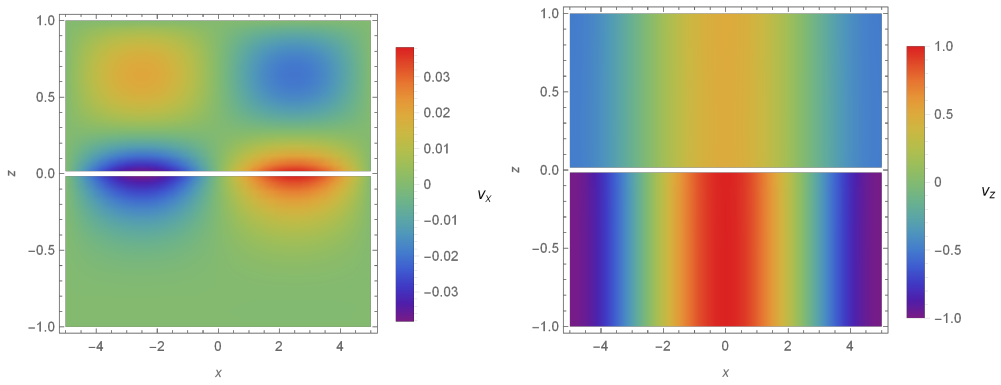

(a) sharp interface – classical traction jump

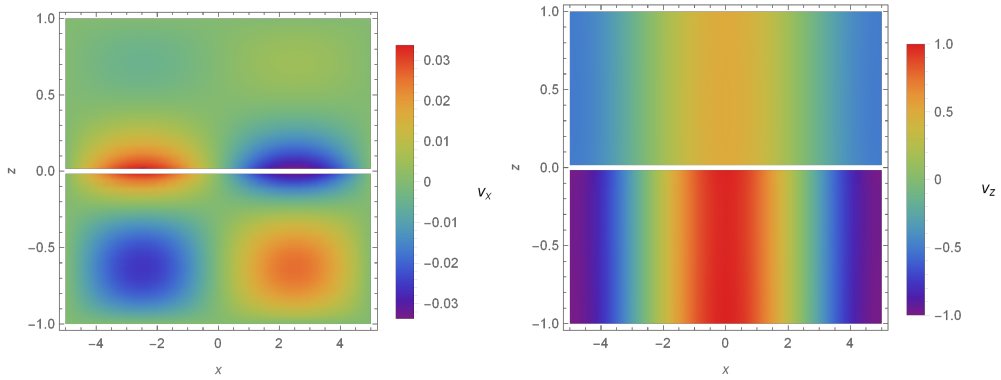

(b) sharp interface – Chambat traction jump

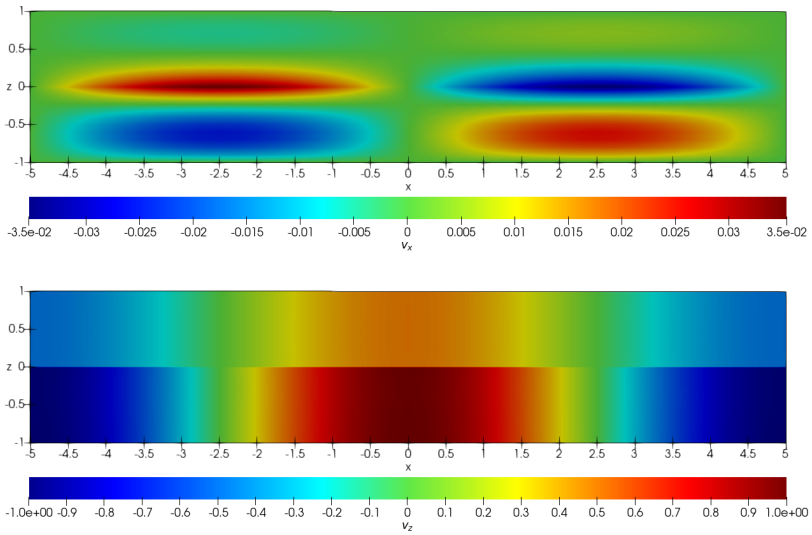

(c) diffuse interface

Figure 2.3: Planar flow velocity fields in the sharp and diffuse interface approaches. The two versions of the flow profile in the sharp interface model represent the classical and Chambat traction jump conditions. It is evident that the numerical solution yields results inconsistent with the theoretically predicted behavior assuming continuous traction, which can be seen here in the differences between the x-components of the respective velocity fields. This inconsistency can be catered for by introducing a nontrivial jump in traction attributed by Chambat et al. [2014] to dynamic surface tension. Note that all plotted quantities are considered non-dimensional and without explicit physical units.

Chapter 3

Dynamic Surface Tension – Analytical Insights

The conclusion of the previous chapter was that there is indeed a new phenomenon in the form of *dynamic surface tension* that arises when solving the Stokes flow across an interface from the diffuse interface point of view. This chapter aims at giving an insight into the way the nontrivial jump of traction is obtained from the limiting process of the transitional layer thickness going to zero, still using simple enough models to allow fully analytical treatment.

The expression for the traction jump condition (1.18) proposed by Chambat et al. [2014] consists of two terms – one corresponding to the *Marangoni effect* and other to the *Young-Laplace law*. It is therefore illustrative to investigate the properties of the diffuse interface solutions in special geometries, where one of the terms vanishes. Hence, in what follows, we first treat a two-dimensional system with a *planar* interface, where only the Marangoni term is nontrivial, and then shift our focus to a radially symmetric flow across a *spherical* interface, relevant to the Young-Laplace term. Note that the planar system differs slightly from the one treated in the previous chapter, as we are essentially solving the equations in an *unbounded* domain, and we are only interested in the behavior of the solutions near the interface.

The observations made in this chapter will then serve as a starting point for the study of generalized solutions of governing equations in domains with an interface in subsequent chapters.

3.1 Diffuse Interface Solutions for the Planar Interface

In this section, we consider a two-dimensional planar flow (the coordinates being again x and z) with an interfacial layer centered around $z = 0$. We assume that the governing equations (1.14), (1.15) hold everywhere in the (a priori unbounded) domain, including the interface, and take the jump of the xz-component of the Cauchy stress tensor as the limit

$$[\![T_{xz}]\!] = \lim_{\delta \to 0} \int_{-\delta}^{\delta} \frac{\partial T_{xz}}{\partial z} \, \mathrm{d}z, \tag{3.1}$$

assuming its differentiability for any fixed δ. This assumption follows from the assumption of existence of classical solution inside the interface.

In the two-dimensional planar flow, the Cauchy stress tensor given by (1.19) takes the form

$$\mathbb{T} = \begin{bmatrix} T_{xx} & T_{xz} \\ T_{xz} & T_{zz} \end{bmatrix},$$

where

$$\begin{aligned} T_{xx} &= -p + (2\eta + \lambda)\frac{\partial v_x}{\partial x} + \lambda \frac{\partial v_z}{\partial z}, \\ T_{xz} &= \eta \left(\frac{\partial v_z}{\partial x} + \frac{\partial v_x}{\partial z} \right), \\ T_{zz} &= -p + \lambda \frac{\partial v_x}{\partial x} + (2\eta + \lambda)\frac{\partial v_z}{\partial z}. \end{aligned} \tag{3.2}$$

We regularize the jump discontinuities in the density field as well as in the rheology parameters η, λ, using one smooth profile function $f(z)$ for all quantities. We set

$$\frac{1}{\rho}(z) = \frac{1}{\rho_0} f(z), \quad \eta(z) = \eta_0 f(z), \quad \lambda(z) = \lambda_0 f(z). \tag{3.3a}$$

In addition, we prescribe a special nontrivial mass flux and the corresponding velocity field

$$q(x) = q_0 x, \quad \mathbf{v}(x,z) = v_z(x,z)\mathbf{e}_z = \frac{q(x)}{\rho(z)}\mathbf{e}_z. \tag{3.3b}$$

The form of the velocity field above has been chosen mainly for the sake of simplicity and for illustrative purposes. Additional remarks on the scope of this choice are made further on. First, let us verify that this choice of transitional profiles is compatible with the momentum balance equation.

Lemma 3.1. *The forms of field quantities postulated in* (3.3) *define a class of solutions of the momentum balance equation* (1.15) *in the case of two-dimensional planar flow.*

Proof. If we now substitute the transitional profiles (3.3) into the constitutive formulae (3.2), we obtain

$$\begin{aligned} T_{xx} &= -p + \frac{\lambda_0 q(x)}{\rho_0} \left(\frac{f^2}{2} \right)'(z), \\ T_{xz} &= \frac{\eta_0 \dot{q}(x)}{\rho_0} f^2(z), \\ T_{zz} &= -p + \frac{(2\eta_0 + \lambda_0) q(x)}{\rho_0} \left(\frac{f^2}{2} \right)'(z). \end{aligned}$$

In view of the above identities, the momentum balance

$$\frac{\partial T_{xx}}{\partial x} + \frac{\partial T_{xz}}{\partial z} = 0, \quad \frac{\partial T_{xz}}{\partial x} + \frac{\partial T_{zz}}{\partial z} = 0,$$

can be written in the form

$$\frac{\partial p}{\partial x} = \frac{(\lambda_0 + 2\eta_0)\dot{q}(x)}{\rho_0}\left(\frac{f^2}{2}\right)'(z),$$
$$\frac{\partial p}{\partial z} = \frac{2\eta_0\ddot{q}(x)}{\rho_0}\left(\frac{f^2}{2}\right)(z) + \frac{(2\eta_0 + \lambda_0)q(x)}{\rho_0}\left(\frac{f^2}{2}\right)''(z).$$

The first term in the second equation vanishes because q is assumed to be linear.

The compatibility condition for this system to be solvable is the equality of mixed second partial derivatives of p. Taking the z-partial derivative of the first equation and the x-partial derivative of the second yields

$$\frac{\partial^2 p}{\partial z \partial x} = \frac{\partial^2 p}{\partial x \partial z} = \frac{(\lambda_0 + 2\eta_0)\dot{q}(x)}{\rho_0}\left(\frac{f^2}{2}\right)''(z),$$

which means that the two equations are compatible and the system is solvable for the proposed transitional profiles. □

Remark. The compatibility condition on the second mixed partial derivatives of pressure in fact requires only that the third derivative of q be trivial. The velocity profile could therefore be defined in a more general form using

$$q(x) = q_0 + q_1 x + q_2 x^2$$

with q_0, q_1, q_2 constants. However, this generalization is of little interest in the context of the studied properties of the flow, which makes the choice of simple linear velocity profile in the x coordinate more reasonable.

Now that we have made sure that the assumption on the form of the field quantities inside the interface is consistent with the momentum balance equation, we can proceed to deriving the jump of the xz-component of the Cauchy stress tensor. We shall compare the results obtained via the definition of the jump (3.1) to the results from substituting the profiles (3.3) into the Chambat et al. [2014] form of the traction jump

$$[\![T_{xz}]\!] = \lim_{\delta\to 0} 2\frac{\partial}{\partial x}\left(\rho v_z \int_{-\delta}^{\delta} \eta \frac{\partial}{\partial z}\left(\frac{1}{\rho}\right) \mathrm{d}z\right).$$

First, let us use the definition of the jump. Substituting the transitional profiles into Equation (3.1) leads to

$$\begin{aligned}[\![T_{xz}]\!] &= \lim_{\delta\to 0}\int_{-\delta}^{\delta} \frac{\partial T_{xz}}{\partial z}\,\mathrm{d}z = \\ &= \frac{2\eta_0\dot{q}(x)}{\rho_0}\lim_{\delta\to 0}\int_{-\delta}^{\delta}\left(\frac{f^2}{2}\right)'(z)\,\mathrm{d}z = \\ &= \frac{\eta_0\dot{q}(x)}{\rho_0}[\![f^2]\!].\end{aligned}$$

On the other hand, the Chambat et al. [2014] jump condition in conjunction with the assumed form of regularization of discontinuities in the relevant physical

quantities yields

$$\begin{aligned}\llbracket T_{xz} \rrbracket &= \lim_{\delta\to 0} 2\frac{\partial}{\partial x}\left(\rho v_z \int_{-\delta}^{\delta} \eta \frac{\partial}{\partial z}\left(\frac{1}{\rho}\right) \mathrm{d}z\right) = \\ &= \frac{2\eta_0 \dot{q}(x)}{\rho_0} \lim_{\delta\to 0} \int_{-\delta}^{\delta} \left(\frac{f^2}{2}\right)' (z)\, \mathrm{d}z = \\ &= \frac{\eta_0 \dot{q}(x)}{\rho_0} \llbracket f^2 \rrbracket.\end{aligned}$$

It is therefore clear that these two methods of deriving the jump conditions are equivalent in the special case where the velocity and density fields as well as the viscosity coefficients inside the transitional layer are given by formulae from Equations (3.3). Thus, the sharp interface limit of planar diffuse interface solutions does not lead to continuous traction, but on the contrary it induces a nontrivial jump that can be interpreted as the Marangoni term of dynamic surface tension inside the interface.

Remark. The purpose of the model given by transitional profiles (3.3) is primarily to illustrate the diffuse interface approach and the results it yields in relation to the traction jump condition proposed by Chambat et al. [2014]. Hence, while this model generates a class of admissible solutions of the momentum balance system of equations in a relatively straightforward way, it is quite restrictive in terms of scaling of discontinuities in respective quantities. By specifying the profile via a multiple of a single smooth function $f(z)$, the model essentially leaves just one degree of freedom to each quantity.

A more general model would involve specifying two parameters for each discontinuous physical quantity, one describing its *magnitude* and other scaling its *jump*. This type of model will be investigated for the radially symmetric flow problem in the next section.

In the following chapter, we suggest that the idea of regularization of discontinuities presented above using a specific profile function f can be generalized to allow a mathematically sensible treatment of nonlinear singular terms such as those seen in the traction jump by Chambat et al. [2014], where the product $\eta\partial_z(1/\rho)$ behaves as a product of a Heaviside function by a Dirac mass at its point of discontinuity in the limit $\delta \to 0$.

3.2 Diffuse Interface Solutions for the Spherical Interface

The second special case we treat here is the case of a *spherically symmetric* velocity field *diverging from a point*. It is clearly efficient to describe the problem in spherical coordinates (r, θ, ϕ). Since the problem is supposed to be radially symmetric, we assume the following form of the field quantities of interest:

$$\mathbf{v} = v(r)\mathbf{e}_r, \quad \rho = \rho(r), \quad \lambda = \lambda(r), \quad \eta = \eta(r). \tag{3.4}$$

Using the expressions for the action of vector operators on functions of spherical coordinates

$$\operatorname{div}\mathbf{v} = \operatorname{div}\left(v(r)\mathbf{e}_r\right) = \frac{1}{r^2}\frac{\mathrm{d}}{\mathrm{d}r}(r^2 v),$$
$$\frac{1}{2}\left[\nabla\mathbf{v} + (\nabla\mathbf{v})^T\right] = \frac{\mathrm{d}v}{\mathrm{d}r}\mathbf{e}_r \otimes \mathbf{e}_r + \frac{v}{r}\left(\mathbf{e}_\theta \otimes \mathbf{e}_\theta + \mathbf{e}_\phi \otimes \mathbf{e}_\phi\right),$$

found, e.g., in the book by [Martinec, 2010, p. 233 – 238], it can be deduced that the Cauchy stress tensor is given by

$$\mathbb{T} = \begin{bmatrix} T_{rr} & 0 & 0 \\ 0 & T_{\theta\theta} & 0 \\ 0 & 0 & T_{\phi\phi} \end{bmatrix},$$

where

$$\begin{aligned} T_{rr} &= -p + 2\lambda\frac{v}{r} + (\lambda + 2\eta)\frac{\mathrm{d}v}{\mathrm{d}r}, \\ T_{\theta\theta} = T_{\phi\phi} &= -p + 2(\lambda + \eta)\frac{v}{r} + \lambda\frac{\mathrm{d}v}{\mathrm{d}r}. \end{aligned} \tag{3.5}$$

The next step is to substitute the explicit form of $\mathbb{T}$ into the momentum balance equation (1.15). The vector analysis formulae presented by Martinec [2010] yield

$$\begin{aligned} \operatorname{div}\mathbb{T} = &\left[\frac{1}{r^2}\frac{\partial}{\partial r}(r^2 T_{rr}) - \frac{1}{r}(T_{\theta\theta} + T_{\phi\phi})\right]\mathbf{e}_r + \\ &+ \left[\frac{1}{r\sin\theta}\frac{\partial}{\partial\theta}(\sin\theta T_{\theta\theta}) - \frac{\cot\theta}{r}T_{\phi\phi}\right]\mathbf{e}_\theta + \frac{1}{r\sin\theta}\frac{\partial T_{\phi\phi}}{\partial\phi}\mathbf{e}_\phi = \mathbf{o}. \end{aligned} \tag{3.6}$$

In view of the assumptions (3.4) on the velocity and density fields and on the viscosity coefficients, the only term in the presently considered form of the Cauchy stress tensor that may depend on the angular coordinates θ, ϕ is the pressure. This issue is addressed in the following lemma.

Lemma 3.2. *In a radial quasi-static Stokes flow diverging from a point, the pressure field is* radial*, i.e., $p = p(r)$.*

Proof. The ϕ-component of Equation (3.6) reads

$$\frac{1}{r\sin\theta}\frac{\partial T_{\phi\phi}}{\partial\phi} = -\frac{1}{r\sin\theta}\frac{\partial p}{\partial\phi} = 0,$$

therefore the pressure cannot depend on ϕ. Moreover, if we take its θ-component, then it is clear from the simple manipulations

$$\frac{1}{r\sin\theta}\frac{\partial}{\partial\theta}(\sin\theta T_{\theta\theta}) - \frac{\cot\theta}{r}T_{\phi\phi} = \ = \frac{\cot\theta}{r}\underbrace{\left[T_{\theta\theta} - T_{\phi\phi}\right]}_{=0} + \frac{1}{r}\frac{\partial T_{\theta\theta}}{\partial\theta} = -\frac{1}{r}\frac{\partial p}{\partial\theta} = 0$$

that the pressure must be independent of θ, too. Consequently, the pressure field $p = p(r)$ is radial. □

If we now rearrange the remaining terms in Equation (3.6) and express the angular components of $\mathbb{T}$ as

$$T_{\theta\theta} = T_{\phi\phi} = T_{rr} - 2\eta\frac{\mathrm{d}v}{\mathrm{d}r} + 2\eta\frac{v}{r},$$

we can conclude that the mass balance equation for the radial flow reduces to an ODE for T_{rr}

$$\frac{\mathrm{d}T_{rr}}{\mathrm{d}r} + \frac{4\eta}{r}\left(\frac{\mathrm{d}v}{\mathrm{d}r} - \frac{v}{r}\right) = 0. \tag{3.7}$$

As for the mass balance equation (1.14), it can be integrated directly as follows:

$$\operatorname{div}(\rho\mathbf{v}) = \frac{1}{r^2}\frac{\mathrm{d}}{\mathrm{d}r}(r^2\rho v) = 0 \implies \rho v = \frac{C}{r^2}, \tag{3.8}$$

where C is a constant to be determined.

For the traction jump (jump of the rr-component of the Cauchy stress tensor), the aim is to compare the discontinuity implied by the limiting behavior of the diffuse interface solution to the Chambat et al. [2014] jump condition (1.18), which reduces to

$$[\![T_{rr}]\!] = -4\frac{\rho v}{R}\lim_{\delta\to 0}\int_{R-\delta}^{R+\delta}\eta\frac{\mathrm{d}}{\mathrm{d}r}\left(\frac{1}{\rho}\right)\mathrm{d}r \tag{3.9}$$

in the radial case.

Suppose we model the interface as a spherical surface located at $r = R$. As for the two-dimensional planar flow, we proceed to treat the interface as a *transitional layer* corresponding to the interval $[R-\delta, R+\delta]$ for some small value of δ. Next, we regularize the discontinuities in both the density and the viscosity fields via the same *transitional profile function* $\chi(r)$ as

$$\frac{1}{\rho}(r) = g + g_\Delta\,\chi(r), \quad \eta(r) = f + f_\Delta\,\chi(r), \tag{3.10}$$

where f, f_Δ, g, g_Δ are assumed constant. Substituting these profiles into Equation (3.7) along with the expression for velocity from Equation (3.8) then yields

$$\begin{aligned} 0 &= \frac{\mathrm{d}T_{rr}}{\mathrm{d}r} - \frac{4C}{r^3}(f + f_\Delta\,\chi(r))g_\Delta\,\chi'(r) - \frac{12C}{r^4}(f + f_\Delta\,\chi(r))(g + g_\Delta\,\chi(r)) = \\ &= \frac{\mathrm{d}T_{rr}}{\mathrm{d}r} - \frac{4C}{r^3}\left(fg_\Delta\,\chi + \frac{f_\Delta g_\Delta}{2}\chi^2\right)'(r) - \frac{12C}{r^4}(f + f_\Delta\,\chi(r))(g + g_\Delta\,\chi(r)). \end{aligned}$$

The jump condition can then be obtained by integrating the equation, which leads to

$$\begin{aligned} [\![T_{rr}]\!] = &-\lim_{\delta\to 0}\int_{R-\delta}^{R+\delta}\frac{4C}{r^3}\left(fg_\Delta\,\chi + \frac{f_\Delta g_\Delta}{2}\chi^2\right)'(r) + \\ &+\lim_{\delta\to 0}\int_{R-\delta}^{R+\delta}\frac{12C}{r^4}(f + f_\Delta\,\chi(r))(g + g_\Delta\,\chi(r))\,\mathrm{d}r = \\ &= -\frac{4C}{R^3}\left(fg_\Delta[\![\chi]\!] + \frac{f_\Delta g_\Delta}{2}[\![\chi^2]\!]\right) + \\ &+ 12C\underbrace{\lim_{\delta\to 0}\int_{R-\delta}^{R+\delta}\frac{fg_\Delta\,\chi + \frac{f_\Delta g_\Delta}{2}\chi^2 + (f + f_\Delta\,\chi(r))(g + g_\Delta\,\chi(r))}{r^4}\,\mathrm{d}r}_{=0}, \end{aligned} \tag{3.11}$$

where the integral vanishes in the limit due to the regularity of the integrand.

On the other hand, substituting the transitional profiles (3.10) into the jump condition (3.9) proposed by Chambat et al. [2014] gives us

$$[\![T_{rr}]\!] = -4\frac{C}{R^3}\lim_{\delta\to 0}\int_{R-\delta}^{R+\delta}(f + f_\Delta\,\chi(r))g_\Delta\,\chi'(r)\,\mathrm{d}r = -\frac{4C}{R^3}\left(fg_\Delta[\![\chi]\!] + \frac{f_\Delta g_\Delta}{2}[\![\chi^2]\!]\right),$$

which is the same result as in Equation (3.11).

The results of this section confirm the hypothesis postulated by Chambat et al. [2014] that, in the limit $\delta \to 0$, the diffuse interface approach does not correspond to the classical requirement of continuous traction across the interface in the case of a radially symmetric flow. Instead, the limiting behavior of the diffuse interface solution induces a discontinuity in the rr-component of the Cauchy stress tensor similar to the Young-Laplace law and attributed by Chambat et al. [2014] to dynamic surface tension inside the interface.

Chapter Summary The goal of this chapter was to provide an insight into the behavior of diffuse interface solutions of the quasi-static Stokes flow in two special cases, planar and radial, and to illustrate how the respective terms of the dynamic surface tension introduced by Chambat et al. [2014] are indeed an intrinsic property of the diffuse interface model. In what follows, we shall study the sharp interface as a limit of the diffuse interface approach in a mathematically rigorous framework of generalized functions well-suited to the type of equations encountered here.

Chapter 4

Generalized Solutions of the Governing Equations

In what follows, we shall extend the ideas illustrated on the special cases treated in Chapter 3 to a more general mathematical framework. The mathematical theory used to interpret the Stokes flow problem enables further generalizations of the setting, which will be discussed.

Since we are interested in a system where multiple known and unknown variables are expected to be discontinuous, it is natural to seek some kind of *generalized* solutions for the governing equations. These are usually constructed using the *linear distribution theory* introduced by Schwartz [1950]. Despite being very abstract mathematically, the theory of distributions has clear physical motivation, whether it is the mathematical treatment of point charges in classical electrodynamics, or the notion of a localized particle in quantum mechanics.

However, as was shown very early on by Schwartz [1954], the linear theory with its intuitive properties fails to cater for nonlinear operations as simple as distribution multiplication. This assertion, referred to as the *Schwartz impossibility result*, essentially means that any nonlinear theory of generalized functions necessarily has to lose intuitive properties like consistency of multiplication of continuous functions. There were several attempts to overcome this difficulty, but the approach of Jean François Colombeau, presented for example by Rosinger [1987], has proved to be one of the more convenient by its numerous applications, namely in theory of nonlinear elasticity (cf. Průša and Rajagopal [2016]).

We start the chapter by stating fundamental definitions and properties of the *Colombeau algebra*. Then we take the radial stationary Stokes problem discussed in Section 3.2 and reinterpret the equation in terms of the newly introduced generalized framework. To end the chapter, a numerical illustration of the derived results is given by investigating the convergence of the diffuse interface solutions to the sharp interface model with the formally derived traction jump.

4.1 Review of the Colombeau Algebra of Generalized Functions

We first give a brief outline of the theoretical framework used throughout the rest of the chapter. The definitions as well as parts of the notation are taken from

Rosinger [1987].

The starting point for Colombeau's construction of nonlinear theory of generalized functions is the fact that any distribution $T \in \mathcal{D}'$ can be approximated by functions from C^∞ via convolutions with compactly supported smooth functions $\phi_\varepsilon \in \mathcal{D}$ such that $\lim_{\varepsilon \to 0^+} \phi_\varepsilon = \delta$ in $\mathcal{D}'$, where δ is the Dirac distribution. These functions are sometimes called *smoothing kernels*. The key here is to define appropriate classes of smooth approximations in order to obtain a differential algebra with the corresponding quotient structure.

4.1.1 Colombeau Algebra Definition

To restrict the choice of smoothing kernels, let us define the following *index sets*.

Definition 4.1. For $m \in \mathbb{N}$, define Φ_m as the set of all functions $\phi \in \mathcal{D}(\mathbb{R}^n)$ satisfying

$$\int_{\mathbb{R}^n} \phi(x)\,\mathrm{d}x = 1 \quad \text{and} \quad \forall \alpha \in \mathbb{N}_0^n, 1 \leq |\alpha| \leq m : \int_{\mathbb{R}^n} x^\alpha \phi(x)\,\mathrm{d}x = 0,$$

where α is a multiindex.

It is easy to see that the inclusions

$$\Phi_1 \supset \Phi_2 \supset \cdots \supset \Phi_m \supset \cdots$$

hold, which leads us to define the *basic index set* as $\Phi := \Phi_1$. The object used to construct the Colombeau algebra is $\mathcal{E}[\mathbb{R}^n] := (C^\infty(\mathbb{R}^n))^\Phi$, i.e., the space of "sequences" of C^∞ functions "indexed" by functions from Φ. The notation we use further on refers to the elements of $\mathcal{E}[\mathbb{R}^n]$ as the mappings

$$f : \Phi \times \mathbb{R} \ni (\phi, x) \mapsto f(\phi, x) \in \mathbb{C}.$$

For the sake of convenience, we denote

$$\psi_\varepsilon(x) := \frac{1}{\varepsilon^n} \psi\left(\frac{x}{\varepsilon}\right), \quad \forall x \in \mathbb{R}^n,$$

where $\psi \in \mathcal{D}(\mathbb{R}^n)$ is arbitrary such that $\int_{\mathbb{R}^n} \psi = 1$ and $\varepsilon > 0$.

The construction itself consists of three steps. First, we define an appropriate *subalgebra* in $\mathcal{E}[\mathbb{R}^n]$. Then, we find an *ideal* in that subalgebra. Finally, the Colombeau algebra itself is defined as the quotient of these two objects.

Definition 4.2. Let $\mathcal{A}$ be the subalgebra in $\mathcal{E}[\mathbb{R}^n]$ consisting of all $f \in \mathcal{E}[\mathbb{R}^n]$ such that

$$\begin{gathered} \forall K \subset \mathbb{R}^n \text{ compact}, \forall \alpha \in \mathbb{N}_0^n, \exists m \in \mathbb{N} : \forall \phi \in \Phi_m, \exists \eta, c > 0 : \\ |D^\alpha f(\phi_\varepsilon, x)| \leq \frac{c}{\varepsilon^m}, \quad \forall x \in K, \forall \varepsilon \in (0, \eta), \end{gathered} \tag{4.1}$$

where D^α is the usual partial derivative of the C^∞ function $\mathbb{R}^n \ni x \mapsto f(\phi_\varepsilon, x) \in \mathbb{C}$.

Let $\mathcal{I}$ be the ideal in $\mathcal{A}$ given by $f \in \mathcal{A}$ such that

$$\begin{gathered} \forall K \subset \mathbb{R}^n \text{ compact}, \forall \alpha \in \mathbb{N}_0^n, \exists l \in \mathbb{N}, \exists b \in B : \\ \forall m \in \mathbb{N}, m \geq l, \forall \phi \in \Phi_m, \exists \eta, c > 0 : \\ |D^\alpha f(\phi_\varepsilon, x)| \leq c\varepsilon^{b(m)-l}, \quad \forall x \in K, \forall \varepsilon \in (0, \eta), \end{gathered} \tag{4.2}$$

where we have denoted

$$B := \left\{ b : \mathbb{N} \to (0, +\infty);\ b \text{ increasing},\ \lim_{m\to\infty} b(m) = +\infty \right\}.$$

The *Colombeau algebra of generalized functions* is then defined by the quotient structure $\mathcal{G}(\mathbb{R}^n) := \mathcal{A}/\mathcal{I}$.

The interpretation of the definition above is the following. The ideal $\mathcal{I}$ has the role of the null element in the Colombeau algebra. Indeed, the condition (4.2) requires that all derivatives of each $f \in \mathcal{I}$ converge uniformly to zero as $\varepsilon \to 0^+$. Furthermore, the convergence has to be faster for smoothing kernels with more vanishing moments, hence the increasing sequence $b(m)$ in (4.2). It can easily be shown (cf. [Rosinger, 1987, p. 59]) that $\mathcal{I}$ is not an ideal in $\mathcal{E}[\mathbb{R}^n]$. It is thus necessary to define a subalgebra in $\mathcal{E}[\mathbb{R}^n]$ compatible with the structure of $\mathcal{I}$. This is ensured by the condition (4.1) in the definition of $\mathcal{A}$. The Colombeau algebra itself is then defined as the space of equivalence classes with respect to $\mathcal{I}$, i.e., two functions from $\mathcal{A}$ are considered equal in $\mathcal{G}$ provided that their difference is an element of $\mathcal{I}$.

Remark. The elements of $\mathcal{A}$ are sometimes called *moderate* generalized functions, and the elements $\mathcal{I}$ are called *null* generalized functions (cf. Průša and Rajagopal [2016]).

By definition, $\mathcal{G}(\mathbb{R}^n)$ is an associative and commutative algebra. It can also be equipped with differential structure via the *partial derivative operators* $D^\alpha : \mathcal{G}(\mathbb{R}^n) \to \mathcal{G}(\mathbb{R}^n)$, $\alpha \in \mathbb{N}_0^n$ defined by

$$D^\alpha(f + \mathcal{I}) := D^\alpha f + \mathcal{I}, \quad \forall \alpha \in \mathbb{N}_0^n,\ \forall f \in \mathcal{A}. \tag{4.3}$$

Clearly, the operators D^α are linear and satisfy the Leibniz product rule.

4.1.2 Embeddings

The next logical step is to determine the representation of particular classes of functions or distributions in the Colombeau algebra and investigate their compatibility with nonlinear operations, namely multiplication. We introduce the three special cases that will be useful in the following sections.

First, consider the embedding $C^\infty \subset \mathcal{G}$ defined by the mapping

$$C^\infty(\mathbb{R}^n) \ni f \mapsto \widetilde{f} + \mathcal{I} \in \mathcal{G}(\mathbb{R}^n), \tag{4.4}$$

where

$$\widetilde{f}(\phi, x) := f(x), \quad \forall \phi \in \Phi,\ \forall x \in \mathbb{R}^n. \tag{4.5}$$

Thus, the representation of an arbitrary function from C^∞ in Colombeau algebra is the function itself.

Next, the embedding $C^0 \subset \mathcal{G}$ is defined by the mapping

$$C^0(\mathbb{R}^n) \ni f \mapsto \overline{f} + \mathcal{I} \in \mathcal{G}(\mathbb{R}^n), \tag{4.6}$$

where

$$\overline{f}(\phi, x) := \int_{\mathbb{R}^n} f(x + y)\phi(y)\,\mathrm{d}y = \int_{\mathbb{R}^n} f(y)\phi(y - x)\,\mathrm{d}y, \quad \forall \phi \in \Phi,\ \forall x \in \mathbb{R}^n. \tag{4.7}$$

Finally, define the embedding $\mathcal{D}' \subset \mathcal{G}$ by the mapping

$$\mathcal{D}'(\mathbb{R}^n) \ni T \mapsto f_T + \mathcal{I} \in \mathcal{G}(\mathbb{R}^n), \tag{4.8}$$

where

$$f_T(\phi, x) := T_y(\phi(y - x)), \quad \forall \phi \in \Phi, \forall x \in \mathbb{R}^n. \tag{4.9}$$

Note that the embedding (4.6) is a special case of the embedding (4.8), since (4.9) reduces to (4.7) for a regular distribution T generated by a continuous function f.

As argued by Rosinger [1987], the following embedding properties follow trivially from the above constructions.

Theorem 4.3. (i) *The embedding $C^\infty(\mathbb{R}^n) \subset \mathcal{G}(\mathbb{R}^n)$ is an embedding of differential algebras and the function 1 is the unit in the algebra $\mathcal{G}(\mathbb{R}^n)$.*

(ii) *The embedding $C^0(\mathbb{R}^n) \subset \mathcal{G}(\mathbb{R}^n)$ is an embedding of vector spaces.*

(iii) *The embedding $\mathcal{D}'(\mathbb{R}^n) \subset \mathcal{G}(\mathbb{R}^n)$ is an embedding of vector spaces that extends the distributional partial derivatives. In particular, D^α on $\mathcal{G}(\mathbb{R}^n)$ coincides with the usual partial derivative D^α of smooth functions when restricted to $C^l(\mathbb{R}^n)$, $l \in \mathbb{N} \cup \{\infty\}$, $l \geq |\alpha|$.*

4.1.3 Generalized Complex Numbers

In J. F. Colombeau's theory, a generalized function is represented by an entire class of mappings from $\Phi \times \mathbb{R}^n$ to $\mathbb{C}$ that are equivalent in the sense of the definition of the ideal $\mathcal{I}$. Consequently, the definition of the *value* of such generalized functions requires a similar structure on the field of complex numbers. This is the main motivation behind the following definition of *generalized complex numbers*.

In analogy with the construction of the algebra $\mathcal{G}(\mathbb{R}^n)$, the starting point is the algebra $\mathcal{E}_0 := \mathbb{C}^\Phi$.

Definition 4.4. Let $\mathcal{A}_0$ be the subalgebra in $\mathcal{E}_0$ consisting of all $h \in \mathcal{E}_0$ such that

$$\exists m \in \mathbb{N} : \forall \phi \in \Phi_m, \exists \eta, c > 0 : |h(\phi_\varepsilon)| \leq \frac{c}{\varepsilon^m}, \quad \forall \varepsilon \in (0, \eta). \tag{4.10}$$

Let $\mathcal{I}_0$ be the ideal in $\mathcal{A}_0$ given by $h \in \mathcal{A}_0$ such that

$$\begin{gathered} \exists l \in \mathbb{N}, \exists b \in B : \forall m \in \mathbb{N}, m \geq l, \forall \phi \in \Phi_m, \exists \eta, c > 0 : \\ |h(\phi_\varepsilon)| \leq c\varepsilon^{b(m)-l}, \quad \forall \varepsilon \in (0, \eta). \end{gathered} \tag{4.11}$$

The associative and commutative algebra $\overline{\mathbb{C}}$ of *generalized complex numbers* is defined by $\overline{\mathbb{C}} := \mathcal{A}_0/\mathcal{I}_0$.

Similar to the embedding of C^∞ functions in the Colombeau algebra, we can define the embedding $\mathbb{C} \subset \overline{\mathbb{C}}$ by the mapping

$$\mathbb{C} \ni z \mapsto \widetilde{z} + \mathcal{I}_0 \in \overline{\mathbb{C}}, \tag{4.12}$$

where $\widetilde{z}(\phi) = z$ for all $\phi \in \Phi$. This embedding is clearly an embedding of algebras (cf. [Rosinger, 1987, p. 70]).

As we will see later on, it is of advantage to define the following *weaker* notion of correspondence between usual and generalized complex numbers.

Definition 4.5. The usual complex number $z \in \mathbb{C}$ is said to be *associated* with the generalized complex number $\overline{z} \in \overline{\mathbb{C}}$, denoted $\overline{z} \vdash z$, if there is a representation $\overline{z} = h + \mathcal{I}_0 \in \overline{\mathbb{C}}$ such that

$$\exists m \in \mathbb{N},\, \forall \phi \in \Phi_m : \quad \lim_{\varepsilon \to 0^+} h(\phi_\varepsilon) = z.$$

Since not every generalized complex number is associated to a usual complex number (see [Rosinger, 1987, p. 70]), it makes sense to introduce the set

$$\overline{\mathbb{C}}_0 := \left\{ \overline{z} \in \overline{\mathbb{C}};\ \exists z \in \mathbb{C} : \overline{z} \vdash z \right\}.$$

With the above construction of generalized complex numbers, it is straightforward to define the *point value* of a generalized function.

Definition 4.6. Let $F = f + \mathcal{I} \in \mathcal{G}(\mathbb{R}^n)$, $f \in \mathcal{A}$ be a generalized function and let $x \in \mathbb{R}^n$. The *value* $F(x)$ of F at x is the generalized complex number

$$F(x) := f_x + \mathcal{I}_0 \in \overline{\mathbb{C}},$$

where $f_x \in \mathcal{A}_0$ is defined by $f_x(\phi) := f(\phi, x)$ for all $x \in \mathbb{R}^n$.

The embeddings introduced in Section 4.1.2 induce the properties of point values in $\mathcal{G}$ summarized in the theorem below. Proofs of these statements can be found in the textbook by [Rosinger, 1987, p. 75 – 77].

Theorem 4.7. (i) *Let $F \in \mathcal{G}(\mathbb{R}^n)$ be given by a C^∞ function, i.e., $F := f \in C^\infty(\mathbb{R}^n) \subset \mathcal{G}(\mathbb{R}^n)$. Then the value of F at $x \in \mathbb{R}^n$* coincides *with the usual function value $f(x) \in \mathbb{C} \subset \overline{\mathbb{C}}$.*

(ii) *Let $F := f \in C^0(\mathbb{R}^n) \subset \mathcal{G}(\mathbb{R}^n)$, $x \in \mathbb{R}$. Then $F(x) \in \overline{\mathbb{C}}_0$ and $F(x) \vdash f(x)$.*

For technical purposes, we also define the notion of integration in Colombeau algebra.

Definition 4.8. Let $F = f + \mathcal{I} \in \mathcal{G}(\mathbb{R}^n)$, $f \in \mathcal{A}$ be a generalized function and let $K \subset \mathbb{R}^n$ be compact. We define the *integral* of F on K as the generalized complex number

$$\int_K F(x)\,\mathrm{d}x := h + \mathcal{I}_0 \in \overline{\mathbb{C}},$$

where

$$h(\phi) := \int_K f(\phi, x)\,\mathrm{d}x, \quad \forall \phi \in \Phi.$$

Let $F \in G(\mathbb{R}^n)$, $\psi \in \mathcal{D}(\mathbb{R}^n)$, $K \subset \mathbb{R}^n$ compact such that $\operatorname{supp}\psi \subset K$. The integral of $\psi \cdot F$ over K (both the product and the integration in the sense of Colombeau algebra) clearly does not depend on K, which allows us to define

$$\int_{\mathbb{R}^n} (\psi \cdot F)(x)\,\mathrm{d}x := \int_K (\psi \cdot F)(x)\,\mathrm{d}x.$$

4.1.4 Coupled Calculus

As we have mentioned at the beginning of this chapter, any effort to extend the linear theory of generalized functions to nonlinear operations is made all but infeasible by the Schwartz impossibility result. This is true for Colombeau algebra, too. Even fairly simple examples illustrate that the structure of $\mathcal{G}$ is compatible neither with the usual product of continuous functions (cf. [Rosinger, 1987, p. 63 – 64]), nor with the multiplication of a distribution by a C^∞ function, which is well-defined in $\mathcal{D}'$ (cf. [Rosinger, 1987, p. 65]).

To account for these inconsistencies, *additional structure* is introduced into the Colombeau algebra in the form of *equivalence relations* weaker than the equality in the sense of $\mathcal{G}$. For the purposes of this thesis, it is especially useful to consider the *equivalence in the sense of association* defined below.

Definition 4.9. A distribution $T \in \mathcal{D}'(\mathbb{R}^n)$ is said to be *associated* with a generalized function $F \in \mathcal{G}(\mathbb{R}^n)$, denoted $F \Vdash T$, if

$$\int_{\mathbb{R}^n} (\psi \cdot F)(x)\,\mathrm{d}x \vdash \int_{\mathbb{R}^n} (\psi \cdot T)(x)\,\mathrm{d}x, \quad \forall \psi \in \mathcal{D}(\mathbb{R}^n),$$

where both products and both integrals are taken in the sense of $\mathcal{G}(\mathbb{R}^n)$.

Two generalized functions $F_1, F_2 \in \mathcal{G}(\mathbb{R}^n)$ are said to be *associated*, denoted $F_1 \approx F_2$, if $F_2 - F_1 \Vdash 0$.

The above introduced *weaker* concept of equivalence of generalized functions has several convenient properties and a few drawbacks that are listed below. Some of the properties are trivial consequences of the construction of $\mathcal{G}$ and the definition of equivalence in the sense of association. In the case of less direct observations, the reader is invited to refer to Appendix B for their proofs.

(i) Equivalence in the sense of association is compatible with the vector space structure of $\mathcal{G}(\mathbb{R}^n)$ as well as with the partial derivative operators D^α on $\mathcal{G}(\mathbb{R}^n)$ defined by (4.3).

(ii) The equivalence relation $\approx$ reduces to the usual equality $=$ of distributions when restricted to $\mathcal{D}'(\mathbb{R}^n)$.

(iii) If $F_1, F_2 \in \mathcal{G}(\mathbb{R}^n)$ satisfy $F_i = f_i \in C^0(\mathbb{R}^n) \subset \mathcal{G}(\mathbb{R}^n)$, $i = 1, 2$ in the sense of the embedding (4.6) – (4.7), then $F_1 \cdot F_2 \approx T_{f_1 \cdot f_2}$, where the product on the left-hand side is taken in $\mathcal{G}(\mathbb{R}^n)$ and the right-hand side is a Colombeau algebra representation of the regular distribution corresponding to the usual product of continuous functions f_1, f_2.

(iv) Equivalence in the sense of association is *not* compatible with multiplication in $\mathcal{G}(\mathbb{R}^n)$. Namely, it can be shown (cf. Lemma B.5) that while the identities in the sense of association

$$H^q \approx H, \quad (r+1)H^r \cdot \delta \approx \delta$$

hold in $\mathcal{G}$, the product of the left-hand sides of these identities is not associated to the product of the right-hand sides.

The last property shows that a fully general theory of nonlinear generalized functions is hardly feasible, even with an elaborate algebraic structure like $\mathcal{G}$. The following section further supports this claim, introducing the concept of more general nonlinear operations with elements of Colombeau algebra.

4.1.5 Nonlinear Operations

Definition 4.10. A function $\varphi : \mathbb{R}^r \to \mathbb{C}$ is called *slowly increasing* if there exist $a, c > 0$ such that

$$|\varphi(\xi)| \leq c(1 + |\xi|)^a, \quad \forall \xi \in \mathbb{R}^r.$$

The function space $\Theta(\mathbb{R}^r)$ is the differential subalgebra of $C^\infty(\mathbb{R}^r)$ defined by

$$\Theta(\mathbb{R}^r) := \{\varphi \in C^\infty(\mathbb{R}^r);\ \forall \alpha \in \mathbb{N}_0^r : D^\alpha \varphi \text{ slowly increasing}\}.$$

Definition 4.11. Let $F_1, \ldots, F_m \in G(\mathbb{R}^n)$, $m \in \mathbb{N}$, and let $\varphi \in \Theta(\mathbb{R}^m)$. The *nonlinear operation* $\varphi(F_1, \ldots, F_m) \in \mathcal{G}(\mathbb{R}^n)$ is defined by

$$\varphi(F_1, \ldots, F_m) := \varphi(f_1, \ldots, f_m) + \mathcal{I} \in \mathcal{G}(\mathbb{R}^n),$$

where $F_i = f_i + \mathcal{I} \in \mathcal{G}(\mathbb{R}^n)$, $i = 1, \ldots, m$.

According to [Rosinger, 1987, p. 104 – 105], this definition is correct in Colombeau algebra.

The embedding (4.4) implies that, for $F_1, \ldots, F_m$ given by C^∞ functions $f_1, \ldots, f_m$, the nonlinear operation $\varphi(F_1, \ldots, F_m)$ reduces to the usual C^∞ function $\varphi(f_1, \ldots, f_m)$. Similarly, if $f_1, \ldots, f_m \in C^0(\mathbb{R}^n) \subset \mathcal{G}(\mathbb{R}^n)$ in the sense of (4.6), then the generalized function $\varphi(F_1, \ldots, F_m)$ is associated in the sense of Definition 4.9 to the regular distribution induced by $\varphi(f_1, \ldots, f_m)$.

4.2 Application to the Radial Stokes Flow

We are now sufficiently equipped to investigate general solutions of the Stokes flow problem that is at the core of this thesis. For the sake of formal simplicity, as well as relatively straightforward generalization in terms of fluid models, we treat the radially symmetric flow diverging from a point described in Section 3.2.

Recall that the radial case assumes a spherically symmetric velocity field $\mathbf{v} = v(r)\mathbf{e}_r$ and the density ρ, together with the material properties η, λ, are also taken to be r-dependent only. The system is described by the mass balance, which upon integration (cf. (3.8)) yields simply

$$\rho v = \frac{C}{r^2},$$

and the momentum balance that can be expressed in form of the ODE (cf. (3.7))

$$\frac{\mathrm{d}T_{rr}}{\mathrm{d}r} + 4\eta \frac{\mathrm{d}}{\mathrm{d}r}\left(\frac{v}{r}\right) = 0, \quad r \in (0, +\infty).$$

The interface is incorporated into the model by assuming that one or more physical quantities are discontinuous at $r = R$ for a fixed value $R \in (0, +\infty)$.

Purely as a matter of convenience, we introduce the substitution $x := r - R$. The governing equations then read

$$\rho v = \frac{C}{(x + R)^2}, \tag{4.13}$$

$$\frac{\mathrm{d}T_{rr}}{\mathrm{d}x} + 4\eta \frac{\mathrm{d}}{\mathrm{d}x}\left(\frac{v}{x + R}\right) = 0, \quad x \in (-R, +\infty). \tag{4.14}$$

This substitution enables us to describe the discontinuities in field quantities using the *Heaviside function* in its simplest form

$$H(x) = \begin{cases} 0, & x < 0, \\ 1, & x > 0. \end{cases}$$

In what follows, it proves useful to introduce the notation $H_+ := H$, $H_- := 1 - H$. For later reference, we also recall that the *Dirac δ distribution* is defined by

$$\langle \delta, \varphi \rangle = \varphi(0), \quad \forall \varphi \in \mathcal{D}(\mathbb{R}).$$

Remark. Equation (4.13) hints at the fact that the appropriate algebraic structure for the study of this problem is $\mathcal{G}((-R, +\infty))$ rather than $\mathcal{G}(\mathbb{R})$ defined in the previous section, which might lead to inconsistencies when using the properties of Colombeau algebra later on. However, the passage from $\mathcal{G}(\mathbb{R})$ to $\mathcal{G}((-R, +\infty))$ is purely technical, as shown by [Rosinger, 1987, p. 105 – 108]. The exposition of Colombeau algebra on $\mathbb{R}^n$ rather than on arbitrary domains in Section 4.1 was chosen for its illustrative nature without the need for tedious mathematical formalities.

4.2.1 Formal Derivation of the Radial Flow ODE

Similar to the discussion in Section 3.2, our aim here is to investigate the jump of traction T_{rr} in a system with discontinuous density and possibly discontinuous rheology. Thus, as a preliminary step, we need to eliminate the velocity from Equation (4.14) and introduce the inverse density into the equation according to (4.13). This amounts to proving the identity

$$\frac{v}{r} = \frac{C}{r^3} \frac{1}{\rho} \tag{4.15}$$

in $\mathcal{G}((-R, +\infty))$, where we assume that the velocity and inverse density fields are of the form

$$v := \widetilde{v}_1 + \widetilde{v}_2 H_+, \quad \frac{1}{\rho} := \frac{1}{\widetilde{\rho}_1} + \frac{1}{\widetilde{\rho}_2} H_+, \tag{4.16}$$

where $\widetilde{v}_i$, $1/\widetilde{\rho}_i$, $i = 1, 2$ are smooth functions. The identity (4.15) holds trivially for v, $1/\rho$ smooth. Therefore, by considering Equation (4.13) on $(-R, 0)$ and $(0, +\infty)$ respectively, we obtain

$$\frac{\widetilde{v}_i}{r} = \frac{C}{r^3} \frac{1}{\widetilde{\rho}_i}, \quad i = 1, 2,$$

where the equality is understood in the usual context of smooth functions. In order for the substitution $v \leftrightarrow 1/\rho$ to make sense in the Colombeau algebra, the implication

$$\frac{\widetilde{v}_2}{r} = \frac{C}{r^3} \frac{1}{\widetilde{\rho}_2} \quad \text{in } C^\infty((-R, +\infty)) \implies \frac{\widetilde{v}_2}{r} H_+ = \frac{C}{r^3} \frac{1}{\widetilde{\rho}_2} H_+ \quad \text{in } \mathcal{G}((-R, +\infty))$$

is necessary. Fortunately, this is a direct consequence of the embedding $C^\infty \subset \mathcal{G}$ defined by (4.4) – (4.5). We can therefore conclude that the identity (4.15) with

v and $1/\rho$ given by (4.16) holds in $\mathcal{G}((-R,+\infty))$. Hence, we can substitute the mass balance (4.13) into the momentum balance (4.14) to obtain the ODE

$$\frac{\mathrm{d}T_{rr}}{\mathrm{d}x} + \eta \frac{\mathrm{d}}{\mathrm{d}x}\left(\frac{4C}{(x+R)^3}\frac{1}{\rho}\right) \approx 0, \quad x \in (-R,+\infty), \tag{4.17}$$

where the $\approx$ sign means that, instead of strict equality, we are looking for $T_{rr} \in \mathcal{G}((-R,+\infty))$ satisfying the equation in the sense of association.

4.2.2 Interpretation of Nonlinear Terms

We proceed to investigate the meaning and properties in $\mathcal{G}$ of the term

$$\eta \frac{\mathrm{d}}{\mathrm{d}x}\left(\frac{4C}{(x+R)^3}\frac{1}{\rho}\right)$$

that is nonlinear if both density and viscosity are assumed discontinuous. The chief tool in its interpretation is the assumption of some sort of functional relationship between the two discontinuities. In what follows, we first apply this technique to a special case of *polynomial discontinuity* and then discuss a more general approach.

Polynomial Discontinuity

To illustrate the power of the Colombeau algebra framework, let us first discuss a simple case where we assume that the quantities of interest can be expressed as

$$T_{rr} = y + y_\Delta H_+, \quad \eta = f + f_\Delta H_+^q, \quad \frac{4C}{(x+R)^3}\frac{1}{\rho} = g + g_\Delta H_+, \tag{4.18}$$

where f, f_Δ, g, g_Δ are smooth functions and $q \in \mathbb{N}$. The term y_Δ corresponds to the jump of traction. The goal of the following investigation is therefore to derive a theoretical expression for this term.

Substituting these expressions into Equation (4.17) yields

$$\frac{\mathrm{d}y}{\mathrm{d}x} + \frac{\mathrm{d}y_\Delta}{\mathrm{d}x}H_+ + y_\Delta\delta + (f + f_\Delta H_+^q)\left(\frac{\mathrm{d}g}{\mathrm{d}x} + \frac{\mathrm{d}g_\Delta}{\mathrm{d}x}H_+ + g_\Delta\delta\right) \approx 0.$$

If we expand the last term on the left-hand side, we get

$$\begin{aligned}(f + f_\Delta H_+^q)\left(\frac{\mathrm{d}g}{\mathrm{d}x} + \frac{\mathrm{d}g_\Delta}{\mathrm{d}x}H_+ + g_\Delta\delta\right) = \\ = f\frac{\mathrm{d}g}{\mathrm{d}x} + f\frac{\mathrm{d}g_\Delta}{\mathrm{d}x}H_+ + fg_\Delta\delta + f_\Delta\frac{\mathrm{d}g}{\mathrm{d}x}H_+^q + f_\Delta\frac{\mathrm{d}g_\Delta}{\mathrm{d}x}H_+^{q+1} + f_\Delta g_\Delta H_+^q\cdot\delta.\end{aligned}$$

While, as we have mentioned above, the association of generalized functions is not in general compatible with multiplication in the sense of $\mathcal{G}$, it can be shown (cf. Lemma B.3) that the identities

$$H_+^q \approx H_+, \quad H_+^q\cdot\delta \approx \frac{1}{q+1}\delta, \quad \forall q \in \mathbb{N}$$

hold. This means that we can write

$$\begin{aligned}(f + f_\Delta H_+^q)\left(\frac{\mathrm{d}g}{\mathrm{d}x} + \frac{\mathrm{d}g_\Delta}{\mathrm{d}x}H_+ + g_\Delta\delta\right) \approx \\ \approx f\frac{\mathrm{d}g}{\mathrm{d}x} + \left(f\frac{\mathrm{d}g_\Delta}{\mathrm{d}x} + f_\Delta\frac{\mathrm{d}g}{\mathrm{d}x} + f_\Delta\frac{\mathrm{d}g_\Delta}{\mathrm{d}x}\right)H_+ + \left(fg_\Delta + \frac{f_\Delta g_\Delta}{q+1}\right)\delta.\end{aligned} \tag{4.19}$$

We proceed by rewriting the smooth function terms $f\frac{\mathrm{d}g}{\mathrm{d}x}$, $\frac{\mathrm{d}y}{\mathrm{d}x}$ in the form

$$f\frac{\mathrm{d}g}{\mathrm{d}x} \approx f\frac{\mathrm{d}g}{\mathrm{d}x}H_- + f\frac{\mathrm{d}g}{\mathrm{d}x}H_+, \quad \frac{\mathrm{d}y}{\mathrm{d}x} \approx \frac{\mathrm{d}y}{\mathrm{d}x}H_- + \frac{\mathrm{d}y}{\mathrm{d}x}H_+,$$

and thus obtain

$$\begin{aligned}\left(\frac{\mathrm{d}y}{\mathrm{d}x} + f\frac{\mathrm{d}g}{\mathrm{d}x}\right)H_- + \left(\frac{\mathrm{d}}{\mathrm{d}x}(y + y_\Delta) + (f + f_\Delta)\frac{\mathrm{d}}{\mathrm{d}x}(g + g_\Delta)\right)H_+ + \\ + \left(y_\Delta + fg_\Delta + \frac{f_\Delta g_\Delta}{q+1}\right)\delta \approx 0.\end{aligned}$$

This is an algebraic equation in $\mathcal{G}$ that has the form

$$F_1 \cdot H_- + F_2 \cdot H_+ + F_3 \cdot \delta \approx 0 \quad \text{in } \mathcal{G}, \tag{4.20}$$

where F_1, F_2, F_3 are generalized functions corresponding to some smooth functions f_1, f_2, f_3 respectively. It can be shown (cf. Lemma B.6) that the solution of this equation in $\mathcal{G}$ amounts to solving the following three equations:

$$\begin{aligned} f_1(x) &= 0, && \forall x \in (-\infty, 0], \\ f_2(x) &= 0, && \forall x \in [0, +\infty), \\ f_3(0) &= 0. \end{aligned}$$

Applying this to Equation (4.19) yields

$$\frac{\mathrm{d}y}{\mathrm{d}x} + f\frac{\mathrm{d}g}{\mathrm{d}x} = 0 \qquad \text{on } (-R, 0), \tag{4.21}$$

$$\frac{\mathrm{d}}{\mathrm{d}x}(y + y_\Delta) + (f + f_\Delta)\frac{\mathrm{d}}{\mathrm{d}x}(g + g_\Delta) = 0 \qquad \text{on } (0, +\infty), \tag{4.22}$$

$$y_\Delta(0) = -f(0)g_\Delta(0) - \frac{f_\Delta(0)g_\Delta(0)}{q+1}. \tag{4.23}$$

The interpretation of this result is straightforward. Considering the definition of functions y, y_Δ, f, f_Δ, g, and g_Δ, Equations (4.21) and (4.22) mean that the momentum balance equation holds on both subdomains (given by $r < R$ and $r > R$ in the original setting), whereas Equation (4.23) provides the traction jump condition.

Note that in the special case $q = 1$, the derived jump condition is analogous to that derived in Section 3.2. Indeed, instead of considering one specific transition profile function for both inverse density and viscosity, we have now formalized the notion of smooth transition inside the interface and the limiting procedure of decreasing its thickness to zero in the quotient structure of the Colombeau algebra. By expressing the discontinuous quantities via the Colombeau representation of the Heaviside function we are implicitly considering an entire class of transitional profiles. Moreover, the framework of Colombeau algebra enables more general interface behaviors to be considered, as the choice of general $q \in \mathbb{N}$ in the above calculations illustrates.

Generalization by Modelling Argument

While the results of the above discussion seem promising, there is no particular reason to assume a priori that the behavior of discontinuous quantities at the interface can be described by the model (4.18). A slightly more general approach is described by Chambat et al. [2014]. In what the authors call the *modelling argument*, the diffuse interface point of view is taken as a starting point, and it is argued that if we assume that both the density and the viscosity are monotonous functions inside the transitional layer, then there exists a functional relationship $\eta = f(1/\rho)$ connecting these two quantities. This motivates the interpretation of the ill-defined term $\eta(1/\rho)'$[1] via the chain rule as

$$\eta \frac{\mathrm{d}}{\mathrm{d}r}\left(\frac{1}{\rho}\right) = \frac{\mathrm{d}}{\mathrm{d}r} F\left(\frac{1}{\rho}\right),$$

where F is the primitive function of f. If we now assert that this function can be written in the form $F = F_0 + F_\Delta H_+$, then the problematic term can again be thought of as a linear distributional term.

While this is the argument Chambat et al. [2014] use in the formal proof of their proposed jump condition (1.18), it is considered purely in the framework of linear distribution theory, despite the starting point for the argument being clearly beyond this framework. A similar approach is used by Průša and Rajagopal [2016] to treat nonlinear terms in ODEs, this time using the Colombeau algebra. The aim of what follows is to investigate the modelling argument and its correctness in $\mathcal{G}$ in detail.

First, we introduce a generalization of (4.18). While we still assume T_{rr} to have the same form, we postulate

$$\eta = f + f_\Delta(H_+), \quad \frac{4C}{(x+R)^3}\frac{1}{\rho} = g + g_\Delta H_+, \tag{4.24}$$

where f, f_Δ, and g are smooth functions and g_Δ is a constant. The properties of Colombeau algebra dictate that, in order for the above identities to make sense, f_Δ has to be *slowly increasing* in the sense of Definition 4.10.

Although it may seem that this assumption is more restrictive in that g_Δ is no longer allowed to depend on x, it is simply a representation of the fact that we are only interested in the relationship between η and $1/\rho$ "inside" the interface. Furthermore, the choice $f_\Delta(H_+) = f_0 H_+^q$ reduces (4.24) to (4.18).

Substituting (4.24) into the nonlinear term in the ODE (4.17) yields

$$\begin{aligned}\eta \frac{\mathrm{d}}{\mathrm{d}x}\left(\frac{4C}{(x+R)^3}\frac{1}{\rho}\right) &= (f + f_\Delta(H_+)) \cdot \left(\frac{\mathrm{d}g}{\mathrm{d}x} + g_\Delta \delta\right) = \\ &= f\frac{\mathrm{d}g}{\mathrm{d}x} + \frac{\mathrm{d}g}{\mathrm{d}x} f_\Delta(H_+) + f g_\Delta \delta + g_\Delta f_\Delta(H_+)\cdot\delta.\end{aligned}$$

The aim is to interpret the nonlinearity $f_\Delta(H_+)\cdot\delta$ as a derivative of the primitive function to f_Δ with respect to x. This issue is addressed in the following lemma.

[1] This term is problematic in the sense of linear theory of distributions as it is essentially a product of two distributions.

Lemma 4.12. *Let $F_\Delta \in \Theta(\mathbb{R})$ and denote $f_\Delta := F'_\Delta$. Then*

$$\frac{\mathrm{d}}{\mathrm{d}x} F_\Delta(H_+) \approx f_\Delta(H_+) \cdot \delta \tag{4.25}$$

holds in $\mathcal{G}(\mathbb{R})$.

Proof. Throughout the proof, we denote by $g_w \in \mathcal{A}$ the representation of a generalized function $w \in \mathcal{G}$.

Start by expressing the representations of individual terms in $\mathcal{G}(\mathbb{R})$. First,

$$\frac{\mathrm{d}}{\mathrm{d}x} F_\Delta(H_+) = g_{\frac{\mathrm{d}}{\mathrm{d}x}F_\Delta(H_+)} + \mathcal{I} \in \mathcal{G}(\mathbb{R}),$$

and the properties of Colombeau algebra and Definition 4.11 imply that

$$g_{\frac{\mathrm{d}F_\Delta}{\mathrm{d}x}(H_+)}(\phi, x) = \frac{\mathrm{d}}{\mathrm{d}x} g_{F_\Delta(H_+)}(\phi, x) = \frac{\mathrm{d}}{\mathrm{d}x}\left[F_\Delta\left(g_{H_+}(\phi, x)\right)\right], \quad \forall \phi \in \Phi,\, \forall x \in \mathbb{R}$$

holds. Next, we have

$$f_\Delta(H_+) = g_{f_\Delta(H_+)} + \mathcal{I} \in \mathcal{G}(\mathbb{R}),$$
$$g_{f_\Delta(H_+)}(\phi, x) = f_\Delta(g_{H_+}(\phi, x)), \quad \forall \phi \in \Phi,\, \forall x \in \mathbb{R},$$

where the use of Definition 4.11 makes sense because Definition 4.10 implies that if $F_\Delta \in \Theta(\mathbb{R})$, then $f_\Delta \in \Theta(\mathbb{R})$, too. Finally, the embedding (4.8) – (4.9) enables us to write

$$\delta = g_\delta + \mathcal{I} \in \mathcal{G}(\mathbb{R}), \qquad g_\delta(\phi, x) = \phi(-x), \qquad \forall \phi \in \Phi,\, \forall x \in \mathbb{R},$$
$$H_+ = g_{H_+} + \mathcal{I} \in \mathcal{G}(\mathbb{R}), \qquad g_{H_+}(\phi, x) = \int_0^{+\infty} \phi(y - x)\,\mathrm{d}y, \qquad \forall \phi \in \Phi,\, \forall x \in \mathbb{R}.$$

Furthermore, due to the natural properties of the Colombeau algebra, we can write

$$f_\Delta(H_+) \cdot \delta = g_{f_\Delta(H_+)} g_\delta + \mathcal{I} \in \mathcal{G}(R).$$

Our goal is to show that there exists $m \in \mathbb{N}$ such that for all $\phi \in \Phi_m$

$$\lim_{\varepsilon \to 0^+} \int_{-\infty}^{+\infty} \psi(x) \left(\frac{\mathrm{d}}{\mathrm{d}\xi}\left[F_\Delta(g_{H_+}(\phi_\varepsilon, \xi))\right]\Big|_{\xi=x} - f_\Delta(g_{H_+}(\phi_\varepsilon, x))\phi_\varepsilon(-x) \right) \mathrm{d}x = 0$$

holds for arbitrary test functions $\psi \in \mathcal{D}(\mathbb{R})$. This amounts to investigating the behavior of the expression

$$\frac{\mathrm{d}}{\mathrm{d}\xi}\left[F_\Delta(g_{H_+}(\phi_\varepsilon, \xi))\right]\Big|_{\xi=x} - f_\Delta(g_{H_+}(\phi_\varepsilon, x))\phi_\varepsilon(-x) =$$
$$= f_\Delta(g_{H_+}(\phi_\varepsilon, x)) \left[\frac{\mathrm{d}}{\mathrm{d}\xi} g_{H_+}(\phi_\varepsilon, \xi)\Big|_{\xi=x} - \phi_\varepsilon(-x) \right].$$

Differentiating the definition of g_{H_+} with respect to the parameter ξ yields

$$\frac{\mathrm{d}}{\mathrm{d}\xi} g_{H_+}(\phi, \xi) = \frac{\mathrm{d}}{\mathrm{d}\xi} \int_0^{+\infty} \phi(y - \xi)\,\mathrm{d}y =$$
$$= -\int_{-\xi}^{+\infty} \phi'(z)\,\mathrm{d}z =$$
$$= \phi(-\xi),$$

since ϕ is compactly supported by definition. Thus, for all $\phi \in \Phi$ and all $\varepsilon > 0$ we have

$$\frac{\mathrm{d}}{\mathrm{d}\xi} g_{H_+}(\phi_\varepsilon, \xi)\Big|_{\xi=x} - \phi_\varepsilon(-x) = 0$$

and the proof is complete. □

Remark. We have in fact proved an even stronger result, where the equivalence in the sense of association in Equation (4.25) is replaced by equality in $\mathcal{G}(\mathbb{R})$.

The next and final step in the interpretation is to specify the discontinuous structure of $F_\Delta(H_+)$. In order to replicate the thought process behind the modelling argument presented by Chambat et al. [2014], it is necessary to modify the expression for viscosity in (4.24) slightly by assuming

$$\eta = f + f_\Delta(g_\Delta H_+),$$

where f, g_Δ are still constants and f_Δ is a smooth function with a slowly increasing primitive function. It is evident that while this modification does not interfere with the results derived above, it provides the substance of the modelling argument in the form of a relationship between the density and the viscosity. Our goal here is to show that $F_\Delta(g_\Delta H_+) \approx F_\Delta(g_\Delta)H_+$ holds for the primitive function F_Δ of f_Δ. This can be achieved as follows.

If we consider F_Δ and H_+ as functions in their usual sense, then we clearly have

$$F_\Delta(g_\Delta H_+) = \begin{cases} F_\Delta(0), & x < 0, \\ F_\Delta(g_\Delta), & x > 0, \end{cases}$$

$$F_\Delta(g_\Delta)H_+ = \begin{cases} 0, & x < 0, \\ F_\Delta(g_\Delta), & x > 0. \end{cases}$$

If $F_\Delta(0) = 0$, then the regular distributions corresponding to these functions are equal in $\mathcal{D}'(\mathbb{R})$, i.e. $T_{F_\Delta(g_\Delta H_+)} = T_{F_\Delta(g_\Delta)H_+} \in \mathcal{D}'(\mathbb{R})$. It follows from the properties of equivalence in the sense of association (cf. Section 4.1.4) that $F_\Delta(g_\Delta H_+) \approx F_\Delta(g_\Delta)H_+$ holds in $\mathcal{G}(\mathbb{R})$, which is what was to be proved.

To summarize, the modelling argument in the form proposed by Chambat et al. [2014] can be accounted for rigorously in the framework of Colombeau algebra and the full procedure can be summed up to these steps:

(i) Postulate that the behavior of physical quantities at the interface can be described as

$$\eta = f + f_\Delta(g_\Delta H_+), \quad \frac{4C}{(x+R)^3}\frac{1}{\rho} = g + g_\Delta H_+,$$

where f and g are smooth functions, g_Δ is a constant and f_Δ is a slowly increasing function with a slowly increasing primitive function. It is important to choose the particular primitive function F_Δ satisfying $F_\Delta(0) = 0$ for the subsequent parts of the argument to make sense.

(ii) Substitute the above expressions into the momentum balance ODE (4.17) and replace the term involving nonlinear operations with generalized functions H_+ and δ by a derivative of the appropriate primitive function according to the chain rule

$$\frac{\mathrm{d}F_\Delta}{\mathrm{d}x}(g_\Delta H_+) \approx f_\Delta(g_\Delta H_+) \cdot g_\Delta \delta.$$

(iii) Evaluate the above derivative using the identity $F_\Delta(g_\Delta H_+) \approx F_\Delta(g_\Delta) H_+$, which makes sense thanks to the requirement $F_\Delta(0) = 0$ from above. As a result, the ODE (4.17) can be transformed into the form of the algebraic equation (4.20) which is then solved by applying Lemma B.6.

The traction jump condition determined by y_Δ thus obtained reads

$$\boxed{[\![T_{rr}]\!] = y_\Delta = -f(0) g_\Delta - F_\Delta(g_\Delta).} \tag{4.26}$$

To compare it to the expression for traction jump (3.9) proposed by Chambat et al. [2014] we need to evaluate the limit

$$[\![T_{rr}]\!] = -\lim_{\varepsilon \to 0^+} \frac{4C}{R^3} \int_{-\varepsilon}^{+\varepsilon} \eta \frac{\mathrm{d}}{\mathrm{d}x} \left(\frac{1}{\rho} \right) \mathrm{d}x$$

with the expressions for η and $1/\rho$ from (i) above. Note that the expression above has been adjusted for the substitution $r \to x$ used throughout this section for compatibility. Evaluating this limit essentially amounts to properly interpreting the term

$$\eta \frac{\mathrm{d}}{\mathrm{d}x} \left(\frac{4C}{\rho} \right)$$

in Colombeau algebra. If we denote

$$\widetilde{g} := (x + R)^3 g, \quad \widetilde{g}_\Delta := (x + R)^3 g_\Delta,$$

we can write

$$\eta \frac{\mathrm{d}}{\mathrm{d}x} \left(\frac{4C}{\rho} \right) = \eta \frac{\mathrm{d}}{\mathrm{d}x} \left(\widetilde{g} + \widetilde{g}_\Delta H_+ \right) = \eta \frac{\mathrm{d}\widetilde{g}}{\mathrm{d}x} + \eta \frac{\mathrm{d}\widetilde{g}_\Delta}{\mathrm{d}x} H_+ + \eta \widetilde{g}_\Delta \delta.$$

The first two terms on the right-hand side correspond to integrable functions (in the classical sense), which means that their integrals over $(-\varepsilon, +\varepsilon)$ vanish as $\varepsilon \to 0^+$. The third term can be rewritten in $\mathcal{G}$ as

$$\begin{aligned} \eta \widetilde{g}_\Delta \delta &= [f + f_\Delta(g_\Delta H_+)] \widetilde{g}_\Delta \delta \approx \\ &\approx f \widetilde{g}_\Delta \delta + \frac{\widetilde{g}_\Delta}{g_\Delta} f_\Delta(g_\Delta H_+) g_\Delta \delta, \end{aligned} \tag{4.27}$$

provided that $g_\Delta \neq 0$. We already know from previous investigation (see above) that

$$f_\Delta(g_\Delta H_+) g_\Delta \delta \approx F_\Delta(g_\Delta) \delta,$$

and since $\widetilde{g}_\Delta / g_\Delta$ is a smooth function, which makes the multiplication of both sides of the above identity well-defined in $\mathcal{D}'$, the properties of the coupled calculus in

Colombeau algebra ensure that Equation (4.27) is compatible with multiplication by $\widetilde{g}_\Delta/g_\Delta$ in the sense of association. By a similar argument we can show that

$$\frac{\widetilde{g}_\Delta}{g_\Delta}\delta \approx \frac{\widetilde{g}_\Delta(0)}{g_\Delta}\delta, \quad f\widetilde{g}_\Delta\delta \approx f(0)\widetilde{g}_\Delta(0)\delta,$$

which upon substitution into (4.27) yields

$$\eta\widetilde{g}_\Delta\delta \approx R^3\left[f(0)g_\Delta + F_\Delta(g_\Delta)\right]\frac{\mathrm{d}H_+}{\mathrm{d}x}.$$

Substituting this back to the jump condition by Chambat et al. [2014] leads to

$$\begin{aligned}\llbracket T_{rr}\rrbracket &\approx -\lim_{\varepsilon\to 0^+}\frac{1}{R^3}\int_{-\varepsilon}^{+\varepsilon} R^3\left[f(0)g_\Delta + F_\Delta(g_\Delta)\right]\frac{\mathrm{d}H_+}{\mathrm{d}x}\,\mathrm{d}x \approx \\ &\approx -f(0)g_\Delta - F_\Delta(g_\Delta),\end{aligned}$$

which is the desired result identical to Equation (4.26). We have shown that the Chambat et al. [2014] condition is identical to the one derived via Lemma B.6.

4.3 Numerical Solution and the Sharp Interface Limit of the Radial Stokes Flow

The main goal of this section is to illustrate the results of the previous section, namely the expression for the traction jump condition in the case where both the density and the viscosity are discontinuous with the discontinuities parametrized by powers of the Heaviside function, on a numerical solution of the radial Stokes flow mass balance ODE. In what follows, we discuss the details of interpreting the numerical solution in the limit as the thickness of the transitional layer goes to zero, and we show the agreement of theoretical results and numerical experiments.

4.3.1 Problem Setting and Solution Methods

We start by recalling the problem setting. We are interested in the solution of the ODE

$$\frac{\mathrm{d}T_{rr}}{\mathrm{d}r} + \eta\frac{\mathrm{d}}{\mathrm{d}r}\left(\frac{4C}{\rho r^3}\right) = 0, \quad r \in (0, +\infty), \tag{4.28}$$

where we assume that all quantities change across an interface layer centered around $r = R$. In order to mimic the theoretical setup (4.18), we set

$$\eta = f + f_\Delta h^q(r), \quad \frac{4C}{\rho r^3} = g(r) + g_\Delta(r)h(r), \tag{4.29}$$

for $q \in \mathbb{N}$ with h representing an approximation of the Heaviside function (or, more specifically, the Heaviside function translated so that its jump occurs at R as opposed to zero). Inspired by the finite element numerical experiment in Section 2.3, we have chosen to use

$$h(r) := \frac{1}{2}\left(1 + \tanh\frac{r-R}{\varepsilon}\right), \quad \varepsilon > 0.$$

The discontinuous physical quantities that we are approximating have the form

$$\eta = \begin{cases} \eta_1, & r < R, \\ \eta_2, & r > R, \end{cases} \qquad \frac{1}{\rho} = \begin{cases} \dfrac{1}{\rho_1}, & r < R, \\ \dfrac{1}{\rho_2}, & r > R, \end{cases}$$

which leads to the following definition of the terms in Equation (4.29):

$$f := \eta_1, \quad f_\Delta := \eta_2 - \eta_1, \quad g(r) := \frac{4C}{\rho_1 r^3}, \quad g_\Delta(r) := \frac{4C}{r^3}\left(\frac{1}{\rho_2} - \frac{1}{\rho_1}\right).$$

For the purposes of our numerical experiments, the values of relevant parameters are[2]

$$\rho_1 = 1, \quad \rho_2 = 2, \quad \eta_1 = 1, \quad \eta_2 = 2, \quad R = 1, \quad C = 1.$$

Since the purpose of the numerical experiments is to illustrate the validity of result implied by Colombeau algebra theory, the choice of these values is of little physical interest. The discussion of parameters with specific "real-world" meaning can be confined exclusively to the theoretical results, provided that they are in agreement with the numerical experiments.

We used the *Wolfram Mathematica* software to obtain the numerical solution of Equation (4.28). The ODE was solved on the interval $(R - 0.5, R + 0.5)$ and the Cauchy data were set to $T_{rr}(R - 0.1) = 0$. Note that in the case of an ODE as simple as (4.28), the degree of freedom represented by the initial condition (or Cauchy data in general) reduces to simple translation of the solution in the direction of the dependent variable. Because we are only interested in the jump of the solution, the choice of the Cauchy data is effectively irrelevant here.

The solution was computed using the built-in `NDSolveValue` function (cf. Wolfram Research [2012]) with its default parameters. By default, the `NDSolveValue` method chooses the most efficient method for solving the input ODE from all the methods implemented in Wolfram Mathematica. While this certainly obscures the solution process and complicates any detailed interpretation of the results from a numerical standpoint, it is on the other hand convenient in a situation similar to the one presented here, where the exact numerical nature of the computation is not the main concern, and the emphasis is rather on further study of obtained solutions. Hence, we have chosen to use default parameters of this function without deeper investigation.

4.3.2 Definition of the Jump

Once the ODE of interest is solved, the next nontrivial step is the exact definition of jump in the numerical solution which will then be compared to theoretical results. The viscosity and the density being continuous functions of r on the entire solution interval, the traction T_{rr} is also expected to be continuous. This

[2]Similar to the numerical experiment in Chapter 2, we omit the physical units of the parameters to emphasize that the primary purpose of this section is to illustrate the mathematical theory developed in the previous sections. Traction jump for a specific physical system is discussed in the following chapter.

means that, for fixed $\varepsilon > 0$ in the definition of h above, the most straightforward definition of the jump

$$[\![T_{rr}]\!] := \lim_{\xi \to 0} T_{rr}(R+\xi) - T_{rr}(R-\xi)$$

will yield misleading results, as the limit will be equal to zero due to the continuity of T_{rr}. It is therefore natural to resort to a definition of traction jump that somehow depends on the parameter ε representing the "sharpness" of the transitional profiles.

First, define the *variable jump* of a quantity φ as

$$[\![\varphi]\!](\xi) := \varphi(R+\xi) - \varphi(R-\xi).$$

The variable ξ can be thought of as a measure of the interface thickness. It is clear that if the value of ξ is very small, the jump is close to zero for any φ continuous. On the other hand, unless φ is a function approximating a quantity that is piecewise constant, the value of $[\![\varphi]\!](\xi)$ for ξ large enough will not represent the concept of jump across an interface at all correctly. Our goal is therefore to determine the appropriate value of ξ (presumably in relation to ε) to be used for the definition of the jump.

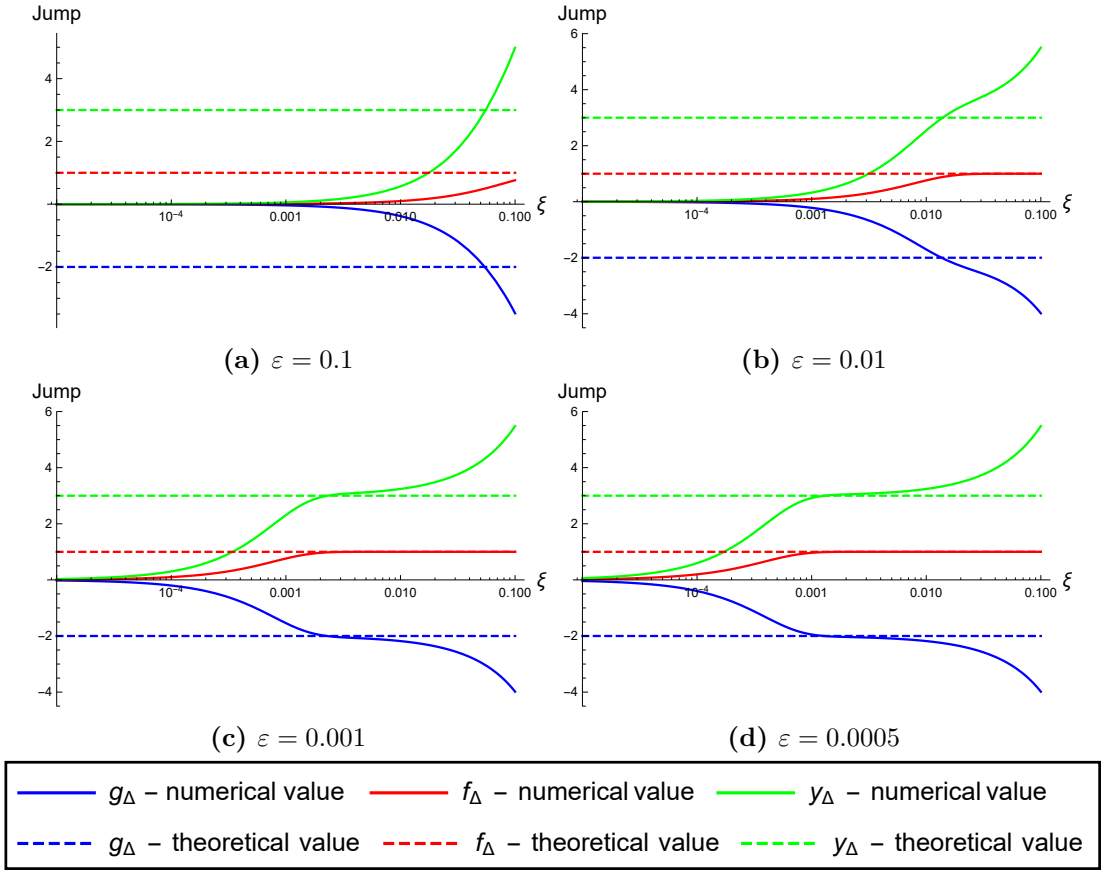

Figure 4.1: Variable jump plots for different values of ε. Besides confirming the expected behavior of the variable jump for extreme values of interface thickness, the above plots pave the way to the correct definition of the jump of the numerical solution of the radial flow ODE. Note that all plotted quantities are considered non-dimensional and without explicit physical units.

In Figure 4.1 we have plotted the functions $[\![\eta]\!](\xi)$ (denoted in the plots as the numerical value of f_Δ), $[\![4C/(\rho r^3)]\!](\xi)$ (denoted in the plots as the numerical

value of g_Δ), and $[\![T_{rr}]\!](\xi)$ (denoted in the plots as the numerical value of y_Δ) for four different values of ε, keeping the value of q in the definition of η fixed at $q = 1$.[3] It is evident from the plots that the comments on the behavior of the variable jump for small and large values of ξ made in the previous paragraph are indeed reasonable. More importantly, though, in Figures 4.1c and 4.1d we can see a plateau appear in between the extreme values of interface thickness. Moreover, the value of the jump at this plateau is in agreement with the theoretical predictions for all three plotted quantities. Hence, we define the *jump of the numerical solution* of the radial Stokes flow ODE (4.28) as

$$[\![T_{rr}]\!]_{\text{num}} := T_{rr}(R + 2\varepsilon) - T_{rr}(R - 2\varepsilon),$$

where ε is the parameter from the definition of h above. The choice of $\xi = 2\varepsilon$ is of course still quite coarse, but as we shall see next, it is already sufficient to show the convergence of the diffuse interface solution to a sharp interface solution with the traction jump prescribed by Chambat et al. [2014].

4.3.3 Convergence Properties of Diffuse Interface Solutions

Equipped with a suitable definition of the jump of numerically computed traction, we proceed to comparing the numerical jump to the one predicted by the considerations of Section 4.2 in the Colombeau algebra framework. Recall that the theoretically derived jump condition (4.23) read

$$[\![T_{rr}]\!] = y_\Delta = \left(f + \frac{f_\Delta}{q+1} \right) g_\Delta(R). \tag{4.30}$$

To study the behavior of the numerical jump with decreasing ε, we solved the ODE (4.28) with viscosity and density profiles given by (4.29), and we computed the numerical jumps $[\![T_{rr}]\!]_{\text{num}}$ according to the definition above for different values of ε and q. The resulting plot is shown in Figure 4.2. It is evident from the plot that the traction jump across the diffuse interface as its thickness goes to zero does indeed converge to the sharp interface limit with discontinuous traction given by (4.30), which, as we have shown in Section 4.2, is the jump condition proposed by Chambat et al. [2014].

Chapter Summary In this chapter we have studied general solutions of the radial Stokes flow across an interface using Colombeau algebra of generalized functions. We have introduced its basic concepts and properties. These were next applied to the interpretation of the modelling argument used to treat nonlinear terms in the relevant governing equations, leading to a result in agreement with the Chambat et al. [2014] traction jump condition. The formally derived results were illustrated by solving the radial Stokes flow in the diffuse interface setting and investigating the limit of the interface thickness going to zero in relation to the traction jump deduced using Colombeau algebra. The possible generalizations and physical implications of these results will be discussed further on.

[3] The labels of quantities in the plots are related to the notation introduced in Section 4.2 and used to derive the theoretical results. Since the emphasis here is on the definition of the jump, $q = 1$ was fixed for simplicity.

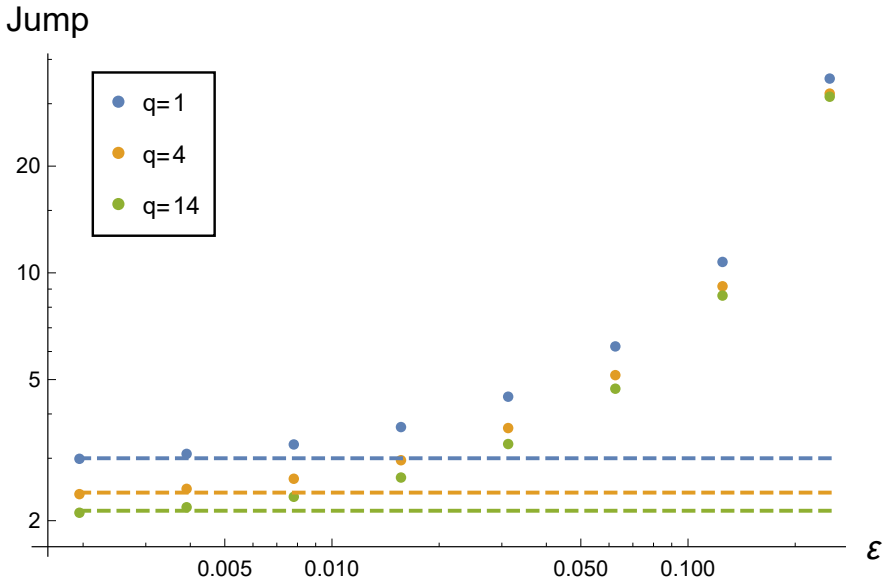

Figure 4.2: Convergence of the diffuse interface numerical solutions to the sharp interface limit. It is clear that as the thickness of the transitional layer in the diffuse interface approach tends to zero, the system converges to a solution with discontinuous traction and its jump is given by the theoretical results of the previous chapter. For illustrative purposes, the convergence rates for $q \in \{1, 4, 14\}$ are given. Similar results can be obtained for other values of q. Note that all plotted quantities are considered non-dimensional and without explicit physical units.

Chapter 5

Discussion and Open Problems

The following chapter is devoted to a broader discussion of the possible generalizations of the work presented in Chapter 4, as well as the physical significance of dynamic surface tension in real-world systems. Rather than a definite account of exact results, the content of this chapter is to be understood as an outline of open problems connected to the subject of the thesis and topics of further research.

5.1 Nonlinear Rheology and Connected Issues

As we have demonstrated in the previous section, the formalism of Colombeau algebra is a very powerful tool in correct mathematical interpretation of generalized solutions of governing equations for a system with an interface. At this point, we make some remarks on possible generalizations of the model system considered in this thesis, and point out the issues connected with such generalizations that are a possible subject of further research.

Besides the extension of the radially symmetric Stokes flow to a flow on a general domain with a general interface, which is presumably of purely formal nature, the most straightforward generalization of the considered system pertains to the fluid rheology. Up to now, we have been working with a linear viscous fluid, whose Cauchy stress tensor is given by Equation (1.19). A slight extension of this constitutive model is the so-called *power law fluid*.

As illustrated, e.g., by Blechta et al. [2020], this model for incompressible fluids is based on the initial view of the Cauchy stress tensor $\mathbb{T}$ being composed of the *mean normal stress* $m\mathbb{I}$ and the *deviatoric stress* $\mathbb{S}$ as $\mathbb{T} = m\mathbb{I} + \mathbb{S}$. The linear rheology (1.19) model used in this thesis, where the incompressibility assumption translates to $\operatorname{div} \mathbf{v} = 0$, is clearly a special case of this prescription with $m = -p$ and $\mathbb{S} = 2\eta\mathbb{D}$, where we have denoted

$$\mathbb{D} \equiv \mathbb{D}(\mathbf{v}) = \frac{1}{2}\left[\nabla\mathbf{v} + (\nabla\mathbf{v})^T\right].$$

According to Blechta et al. [2020], the defining relation of a power law fluid is

$$\mathbb{S} = 2\widetilde{\eta}|\mathbb{D}|^{r-2}\mathbb{D},$$

where $r \in (1, +\infty)$. In relation to the linear model mentioned above, it is natural to define *generalized viscosity* by $\eta_{\mathrm{g}}(|\mathbb{D}|) := \widetilde{\eta}|\mathbb{D}|^{r-2}$, thus obtaining the relation $\mathbb{S} = 2\eta_{\mathrm{g}}\mathbb{D}$.

As for our specific geometrical setting, this reduces to the viscosity η being proportional to some power q of $|\frac{\mathrm{d}v}{\mathrm{d}r}|$. In view of Section 4.2.1, it can be argued that the functional relationship of the viscosity and the spatial derivative of velocity can be transformed to a relationship of the form

$$\eta = \hat{\eta}\left(\frac{\mathrm{d}}{\mathrm{d}r}\left(\frac{1}{\rho}\right)\right),$$

which, if we prescribe discontinuous density, means that the viscosity of the power law fluid is proportional to the generalized function δ^q.

One can assume that substituting this functional relationship even in the simple special case $q = 1$ into the momentum balance ODE (4.17) and performing appropriate manipulations would lead to an algebraic equation similar to

$$F_1 \cdot H_- + F_2 \cdot H_+ + F_3 \cdot \delta + F_4 \cdot \delta^2 \approx 0 \quad \text{in } \mathcal{G}.$$

Note that the purpose of this equation is to illustrate the issues bound to appear in the eventual solution of the generalized model, and we do not specify any information on the exact nature of the smooth functions represented by F_i, $i = 1, \ldots, 4$.

Though it may seem that the addition of the δ^2 term is only a minor complication, it causes on the contrary a fundamental shift in the nature of the equation. The fact that there exists no distribution associated to δ^2 in the sense of Definition 4.9 (cf. Lemma B.4) implies that the stress field T_{rr} cannot have just a simple discontinuous structure, but it may be expected that it contains a δ-like singularity. This shows that even a mathematical tool as powerful as Colombeau algebra faces considerable difficulties when faced with highly singular nonlinear terms.

From a mathematical standpoint, it is also interesting to consider fluid models where the outcome of a procedure similar to the one outlined above is a dependence of viscosity on a bounded monotone function of δ as a Colombeau generalized function. For example, the relation $\arctan \delta$ is well-defined in $\mathcal{G}$ thanks to definitions 4.10 and 4.11 and its behavior may be more convenient in the sense of manipulations in the Colombeau algebra.

The goal of this section was to illustrate that any generalization of the treatment of physical systems with an interface within the Colombeau algebra framework that was introduced in Section 4.2 to more complex fluid rheologies is far from trivial and relies heavily on the mathematical theory beyond the linear distributions introduced by Schwartz [1950]. These generalizations are nevertheless very useful and have numerous practical applications, hence the problems outlined in this section constitute a possible subject of further research.

5.2 Jumps for Particular Physical Systems

To conclude the chapter, we comment briefly on the significance of the results of this thesis in specific real-world systems and discuss their relevance. Recall that throughout the thesis, all the exact values of physical quantities were chosen purely for convenient illustration of the mathematical theory, with less emphasis on the actual physical context. In this way, we have effectively decoupled the mathematical and physical sides of the problem and treated the mathematical

aspect in great detail, especially for the case of radially symmetric flow. The results in the form of the jump condition (4.30) can now be used very conveniently to describe real physical systems. In what follows, we give examples of such systems and discuss the impact the discontinuity in traction has on their behavior.

As argued in Chapter 1, the prototypical physical situation modelled by the set of equations studied in this thesis is the flow of a material across a phase interface. One possible example of this situation is the behavior of ice shells on stellar bodies, such as *Enceladus*, an icy moon of Saturn. Let us apply our theoretical results for the traction jump across a radial interface to this specific example.

Motivated by [Čadek et al., 2019, Table 1], we set the densities of water and ice to $\rho_{\text{water}} = 1010\,\text{kg}\,\text{m}^{-3}$, $\rho_{\text{ice}} = 926\,\text{kg}\,\text{m}^{-3}$ respectively, and take $R = 232.1\,\text{km}$ as the interface radius. We take the viscosity of water as $\eta_{\text{water}} = 1 \times 10^{-3}\,\text{Pa}\,\text{s}$, according to [Myers et al., 2002, Table 1]. As for the viscosity of ice, in the context of glacial dynamics, for example the study by Souček et al. [2015], it is generally taken to have some kind of power law dependence. However, it is argued by Čadek et al. [2019] that the use of a constant value $\eta_{\text{ice}} = 3 \times 10^{14}\,\text{Pa}\,\text{s}$ is appropriate here. The remaining constant to be fixed in order to obtain numerical results is C, which can be interpreted as the mass flux constant. This depends mainly on the specific flow regime and will be set simply to $1\,\text{kg}\,\text{s}^{-1}$ in this case. For the sake of simplicity we also fix $q = 1$ from now on.

Substituting the above values into the radial component of the traction jump given by Equation (4.30) yields

$$[\![T_{rr}]\!] = -\frac{4C}{R^3}\frac{\eta_{\text{ice}} + \eta_{\text{water}}}{2}\left(\frac{1}{\rho_{\text{ice}}} - \frac{1}{\rho_{\text{water}}}\right) \approx -4.3 \times 10^{-6}\,\text{Pa}.$$

For comparison, let us estimate the values of T_{rr} in the ice layer. Equation (3.5) implies the estimate

$$T_{rr}^{(\text{ice})} \simeq \frac{4C\eta_{\text{ice}}}{\rho_{\text{ice}}R^3} \approx 0.0001\,\text{Pa},$$

which is approximately two orders of magnitude higher than the jump itself. In this particular context, the value of the jump is around 5 % of the value of traction in one of the subdomains. While not extremely large, such discontinuity is potentially detectable. However, we only treat the radial component of the jump here, which is expected to be small because of the relatively large radius of the interface. It is possible that the planar component of the jump would be even more significant, although the investigation of this component would demand more precise theoretical results for the planar flow than those presented in the thesis.

While some part of the numerical result above is indeed due to the large radius of Enceladus, it has to be said that the term $1/R^3$ figures in both the approximate calculation of the jump and the estimate of the traction in ice. Thus, the difference in order of magnitude of these two values is influenced more importantly by the values of density and viscosity specific to the system (while the densities of the two substances are quite similar, their viscosities differ considerably). We can therefore conclude that the effect of the traction discontinuity in a phase interface would be more significant for a physical system with different parameters, e.g. higher viscosity of both media or greater difference in densities.

Conclusion

The aim of this thesis was to investigate the stationary Stokes flow of a linearly viscous fluid across an interface and compare the classical assumption of traction continuity to the traction jump condition proposed by Chambat et al. [2014].

After a brief overview in Chapter 1 of the concepts of balance laws and jump conditions, as well as the ways of describing phase interfaces, the results by Chambat et al. [2014] that led to the definition of dynamic surface tension were reproduced in Chapter 2. Despite the simplicity of the considered problem, allowing for fully analytical solution of the governing equations in the usual sense as well as numerical solution via finite element method, we have shown a clear inconsistency between the diffuse interface approximation and the sharp interface limit with continuous traction. In Chapter 3, we have investigated the provenance of the traction discontinuity on analytic diffuse interface solutions in the special cases of planar and radial interfaces.

Chapter 4 introduced the Colombeau algebra of generalized functions as a tool enabling mathematically rigorous derivation of the traction jump condition. An explicit formula for the traction jump was derived for the radially symmetric flow using Colombeau algebra, showing an agreement with the result by Chambat et al. [2014]. The theoretical result was illustrated by numerical experiments studying the convergence properties of the diffuse interface solutions in detail. In Chapter 5, possible generalizations of the model system in the Colombeau algebra framework were outlined as subject of possible future research. At the end, values of expected traction jump were calculated for the particular physical system of Enceladus, icy moon of Saturn.

The conclusion of the work presented here is that, if the governing equations for the quasi-static Stokes flow are assumed valid in the entire domain of interest including the interface, the traction jump discontinuity postulated by Chambat et al. [2014] is indeed the one consistent with the equations, i.e., the assumption of continuous traction across an interface appears to be incorrect. Besides reproducing several results from the paper by Chambat et al. [2014], we have provided here a detailed derivation of the jump condition for the radial flow in the Colombeau algebra framework. This acts not only as a mathematically correct interpretation of the provenance of the traction jump, but also provides a convenient way of calculating the jump explicitly for systems with discontinuous rheology.

While the expression for the traction jump we have derived holds only in the special case of spherical symmetry, the difficulty lying in the transition from this special case to a jump across a general three-dimensional interface is presumably formal rather than conceptual. The Colombeau theory of generalized functions also paves the way to further generalizations of the results obtained here.

The work on the subject of this thesis led to several open questions at almost all stages of its development. While some concern the "practical" side of the thesis, i.e. mathematical derivations or implementation of numerical solutions, others are connected deeply to the very nature of the way interfacial phenomena are described in continuum mechanics.

In discussing the extension of the Colombeau algebra generalized treatment of the governing equations to nonlinear fluids with power law rheology, we have suggested that even the simplest form of power dependence, namely the linear dependence of viscosity on the derivative of the inverse density, leads to mathematical problems lying far beyond the linear theory of distributions and the accurate physical interpretation of the results is complicated at best. This illustrates the difficulty of constructing differential algebras of generalized functions usable in a broad range of physical contexts. On the other hand, the complication itself is a consequence of the assumption that the power law rheology and the balance equations hold inside the interface. A priori, this is not a known fact, and is related to the fundamental description of interfaces that will be discussed below.

As for the finite element solution of the sharp interface planar flow problem mentioned very briefly in Section 2.5, it is a clear example of a simple physical system whose numerical solution is hardly trivial and concise theory regarding its implementation in finite elements is scarce. However, the solution via the finite element method can be envisaged with more complex finite element spaces and different methods of prescribing boundary conditions. The details of this approach are a subject of ongoing research.

The last section in the last chapter of the thesis was devoted to numerical evaluation of the traction jump proposed by Chambat et al. [2014] for concrete physical systems. For Enceladus, the calculated jump was two orders of magnitude smaller than the values of traction in ice. Whether this jump is significant enough to impact the results of numerical models of the ice shell evolution on Enceladus is mainly a question of precision of said models, while our investigation suggests that it is potentially detectable. Nevertheless, physical systems with different parameters may lead to the conclusion that traction discontinuity plays a chief role in the behavior of the solutions of the governing equations.

Finally, note that the underlying assumption for all the arguments leading to the discontinuous traction result is that *the governing equations valid for the homogenous phases hold also inside the interface*. While this assumption seems completely reasonable, it is in fact a philosophical test of the limits of continuum mechanics. The continuous description of physical bodies as an approximation of their discrete structure relies on the interpretation of an infinitesimal volume as *a volume small enough so that the quantities of interest can be assumed constant in that volume up to a reasonable precision, but large enough to contain a sufficient number of discrete particles for the averaged quantities to be relevant*, which is sufficient for description of larger control volumes, but is not trivially satisfied for an interfacial layer. This also puts the matter of viewing the sharp interface as a limit of the diffuse interface with balance laws valid throughout the interface into question. Moreover, it shows that the use of regularized quantities as an approximation of discontinuous problem setting in numerical simulations (e.g. via the level set method) *does* in fact introduce an additional physical phenomenon

in the form of dynamic surface tension into the model.

A breakthrough in this question could be achieved in part by designing a simple experimental setup that would allow to somehow measure the traction jump for a real system with a phase interface, where the influence of the jump condition is expected to be important.

Bibliography

James Ahrens, Berk Geveci, and Charles Law. ParaView: An End-User Tool for Large-Data Visualization. In *The Visualization Handbook*, 2005.

Martin S Alnaes, Jan Blechta, Johan Hake, August Johansson, Benjamin Kehlet, Anders Logg, Chris Richardson, Johannes Ring, E Rognes, and Garth N Wells. The FEniCS Project Version 1 . 5. 3(100):9–23, 2015.

Martin Sandve Alnæs, Anders Logg, Kent Andre Mardal, Ola Skavhaug, and Hans Petter Langtangen. Unified framework for finite element assembly. *International Journal of Computational Science and Engineering*, 4(4):231–244, 2009. ISSN 17427193.

D. M. Anderson, G. B. McFadden, and A. A. Wheeler. Diffuse-Interface Methods in Fluid Mechanics. *Annu. Rev. Fluid Mech.*, 1998.

S. E. Bechtel, M. G. Forest, F. J. Rooney, and Q. Wang. Thermal expansion models of viscous fluids based on limits of free energy. *Physics of Fluids*, 15(9): 2681–2693, 2003. ISSN 10706631.

J. Blechta, J. Malek, and K.R. Rajagopal. On the classification of incompressible fluids and a mathematical analysis of the equations that govern their motion. *SIAM Journal on Mathematical Analysis*, 52(2):1232–1289, 2020.

Ondřej Čadek, Ondřej Souček, Marie Běhounková, Gaël Choblet, Gabriel Tobie, and Jaroslav Hron. Long-term stability of Enceladus' uneven ice shell. *Icarus*, 319(October 2018):476–484, 2019. ISSN 10902643.

Frédéric Chambat, Sylvie Benzoni-Gavage, and Yanick Ricard. Jump conditions and dynamic surface tension at permeable interfaces such as the inner core boundary. *Comptes Rendus - Geoscience*, 346(5-6):110–118, 2014. ISSN 16310713.

Philippe G. Ciarlet. *The Finite Element Method for Elliptic Problems*. Society for Industrial and Applied Mathematics, Philadelphia, 2002.

Valerie Corrieu, Catherine Thoraval, and Yanick Ricard. Mantle dynamics and geoid Green functions. *Geophysical Journal International*, 120(2):516–523, 1995. ISSN 1365246X.

R. Defay, I. Prigogine, and A. Bellemans. *Surface Tension and Adsorption*. Longmans, Green & Co Ltd, London, 1966.

Alexandre Ern and Jean-Luc Guermond. *Theory and Practice of Finite Elements*. Springer, 2004. ISBN 9781441919182.

Wolfram Research, Inc. Mathematica, Version 12.2. URL `https://www.wolfram.com/mathematica`. Champaign, IL, 2020.

Robert C. Kirby. Algorithm 839: FIAT, a new paradigm for computing finite element basis functions. *ACM Transactions on Mathematical Software*, 30(4): 502–516, 2004. ISSN 00983500.

Robert C. Kirby and Anders Logg. A compiler for variational forms. *ACM Transactions on Mathematical Software*, 32(3):417–444, 2006. ISSN 00983500.

Jiří Kopáček. *Matematická analýza nejen pro fyziky II.* MatfyzPress, Prague, 4. edition, 2015. ISBN 978-80-7378-282-5.

Hans Petter Langtangen and Anders Logg. *Solving PDEs in Python: The FEniCS Tutorial*, volume I. Springer Open, 2017. ISBN 0027-8424.

Mats G. Larson and Fredrik Bengzon. *The Finite Element Method: Theory, Implementation, and Applications*. Springer, 2013. ISBN 3642332862.

Dag Lindbo. Finite Element Computations for a Conservative Level Set Method Applied to Two-Phase Stokes Flow, 2006. master thesis.

John R. Lister. The Solidification of Buoyancy-Driven Flow in a Flexible-Walled Channel. Part 2. Continual Release. *Journal of Fluid Mechanics*, 272:45–66, 1994. ISSN 14697645.

Anders Logg and Garth N. Wells. DOLFIN: Automated finite element computing. *ACM Transactions on Mathematical Software*, 37(2):1–27, 2010. ISSN 00983500.

Zdeněk Martinec. *Principles of Continuum Mechanics*. Springer Birkhäuser, 2010. ISBN 9783030053895.

Ctirad Matyska. Mathematical Introduction to Geothermics and Geodynamics, 2005. URL `http://geo.mff.cuni.cz/studium/Matyska-MathIntroToGeothermicsGeodynamics.pdf`. lecture notes.

T. G. Myers and J. Low. An approximate mathematical model for solidification of a flowing liquid in a microchannel. *Microfluidics and Nanofluidics*, 11(4): 417–428, 2011. ISSN 16134982.

T. G. Myers, J. P.F. Charpin, and C. P. Thompson. Slowly accreting ice due to supercooled water impacting on acold surface. *Physics of Fluids*, 14(1):240–256, 2002. ISSN 10706631.

Vít Průša and K R Rajagopal. On the response of physical systems governed by non-linear ordinary differential equations to step input. *International Journal of Non-Linear Mechanics*, 81:207–221, 2016. ISSN 00207462.

K R Rajagopal and L Tao. *Mechanics of Mixtures*. World Scientific, 1995.

Y. Ricard. Physics of Mantle Convection. *Treatise on Geophysics: Second Edition*, 7:23–71, 2015.

Elemér E. Rosinger. *Generalized Solutions of Nonlinear Partial Differential Equations*. North-Holland, Amsterdam, 1987. ISBN 0-444-70310-1.

Kim Sangtae and J. Karrila Seppo. *Microhydrodynamics: Principles and Selected Applications*. Butterworth - Heinemann, 1991. ISBN 0750691735.

Laurent Schwartz. *Théorie des distributions*. Number Tome. 1 in Actualités scientifiques et industrielles. Hermann, Paris, 1950.

Laurent Schwartz. Sur l'impossibilité de la multiplication des distributions. *C. R. Acad. Sci.*, 239:847–848, 1954.

John C Slattery, Leonard Sagis, and Eun-Suok Oh. *Interfacial Transport Phenomena*. Springer, 2 edition, 2007. ISBN 0387384383.

Ondřej Souček, Olivier Bourgeois, Stéphane Pochat, and Thomas Guidat. A 3 Ga old polythermal ice sheet in Isidis Planitia, Mars: Dynamics and thermal regime inferred from numerical modeling. *Earth and Planetary Science Letters*, 426:176–190, 2015. ISSN 0012821X.

Wolfram Research. `NDSolveValue`. Wolfram Language function, 2012. URL `https://reference.wolfram.com/language/ref/NDSolveValue.html`. updated 2019.

Appendix A

Modified Reynolds Transport Theorem

The purpose of this appendix is to provide the proof of the modified Reynolds transport theorem and thus to give an insight into the ways singular surfaces are incorporated into the framework of continuum mechanics. We shall first introduce the geometric context considered, then a modified form of the Gauss integration formula will be proved, proceeding finally to a proof of the modified Reynolds transport theorem. The proof presented here is based on the one given by [Martinec, 2010, p. 44 – 47].

We start by specifying the geometry of the problem we are considering. Let $\omega(t)$ be a control volume inside a continuous body in reference configuration and let $\sigma(t)$ be a singular, non-material surface inside $\omega(t)$ such that $\partial\sigma(t) \subset \partial\omega(t)$. Denote by $\mathbf{n}_\sigma$ the unit normal to $\sigma(t)$ and let $\mathbf{n}_\omega$ denote the unit outward normal to $\omega(t)$. Define subdomains ω_-, ω_+ by

$$\omega(t) = \omega_- \cup \omega_+ \cup \sigma(t),$$

where the vector $\mathbf{n}_\sigma$ is pointing towards ω_+.

For the purposes of the manipulations used in the proofs that follow, we also define surfaces σ_-, σ_+, γ_-, γ_+, and their corresponding unit normal vectors $\mathbf{n}_{\sigma_-}$, $\mathbf{n}_{\sigma_+}$, $\mathbf{n}_{\gamma_-}$, $\mathbf{n}_{\gamma_+}$ in such a way that the conditions

$$\begin{aligned} \lim_{\sigma_-,\sigma_+\to\sigma(t)} \gamma_- \cup \gamma_+ &= \partial\omega(t), \\ \lim_{\sigma_\pm\to\sigma(t)} \mathbf{n}_{\sigma_\pm} &= \mp\mathbf{n}_\sigma, \\ \mathbf{n}_{\gamma_\pm} &= \mathbf{n}_\omega|_{\gamma_\pm} \end{aligned} \tag{A.1}$$

hold. The above described setting is illustrated in Figure A.1.

We denote by $\mathbf{w} = \mathbf{w}(\mathbf{x}, t)$ the Eulerian velocity of the singular surface $\sigma(t)$. Note that since $\sigma(t)$ is supposed to be non-material, this velocity is generally different from the Eulerian velocity $\mathbf{v}(\mathbf{x}, t)$.

Having specified the geometry setting, we continue by proving the following modification of the Gauss integration formula.

Theorem A.1 (modified Gauss integration formula for tensors)**.** *Let ω_-, ω_+, $\sigma(t)$ be as in Figure A.1 and let $\mathbb{A}$ be a tensor field differentiable in $\omega_- \cup \omega_+$. Then*

$$\int_{\omega_-\cup\omega_+} \operatorname{div}\mathbb{A}\,\mathrm{d}x = \int_{\partial\omega(t)} \mathbb{A}\mathbf{n}_\omega\,\mathrm{d}s - \int_{\sigma(t)} [\![\mathbb{A}\mathbf{n}_\sigma]\!]\,\mathrm{d}s. \tag{A.2}$$

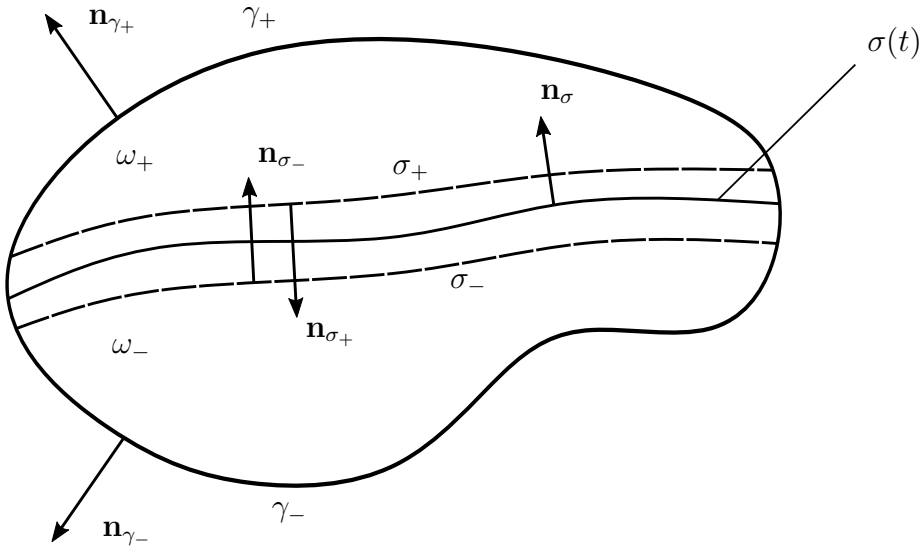

Figure A.1: The geometrical setting used in the proof of the modified Reynolds transport theorem.

Proof. Splitting the integral and applying the regular Gauss integration formula (1.3), we obtain

$$\int_{\omega_-\cup\omega_+} \operatorname{div} \mathbb{A}\,\mathrm{d}x = \lim_{\sigma_-\to\sigma(t)} \left[\int_{\gamma_-} \mathbb{A}\mathbf{n}_{\gamma_-}\,\mathrm{d}s + \int_{\sigma_-} \mathbb{A}\mathbf{n}_{\sigma_-}\,\mathrm{d}s\right] + \\ + \lim_{\sigma_+\to\sigma(t)} \left[\int_{\gamma_+} \mathbb{A}\mathbf{n}_{\gamma_+}\,\mathrm{d}s + \int_{\sigma_+} \mathbb{A}\mathbf{n}_{\sigma_+}\,\mathrm{d}s\right].$$

Applying the conditions (A.1) then yields the desired result (A.2). □

Remark. The corresponding modified formula for vectors

$$\int_{\omega_-\cup\omega_+} \operatorname{div} \mathbf{u}\,\mathrm{d}x = \int_{\partial\omega(t)} \mathbf{u}\cdot\mathbf{n}_\omega\,\mathrm{d}s - \int_{\sigma(t)} [\![\mathbf{u}\cdot\mathbf{n}_\sigma]\!]\,\mathrm{d}s$$

can be derived from Equation (1.2) analogously.

We are now ready to prove the modified version of the Reynolds transport theorem.

Theorem A.2 (modified Reynolds transport theorem)**.** *Let ω_-, ω_+, $\sigma(t)$ be as in Figure A.1 and let ϕ be a scalar or vector defined in $\omega(t)$ that is discontinuous across $\sigma(t)$. Then*

$$\frac{\mathrm{d}}{\mathrm{d}t}\int_{\omega_-\cup\omega_+} \phi\,\mathrm{d}x = \int_{\omega_-\cup\omega_+} \left(\frac{\partial\phi}{\partial t} + \operatorname{div}(\phi\otimes\mathbf{v})\right)\mathrm{d}x - \int_{\sigma(t)} [\![(\phi\otimes(\mathbf{v}-\mathbf{w}))\mathbf{n}_\sigma]\!]\,\mathrm{d}s. \tag{A.3}$$

Sketch of the proof. Splitting the integral and applying the regular Reynolds transport theorem (1.1), as well as the regular Gauss integration formulae (1.2)

and (1.3), we obtain

$$\frac{\mathrm{d}}{\mathrm{d}t}\int_{\omega_-\cup\omega_+}\phi\,\mathrm{d}x=\int_{\omega_-\cup\omega_+}\frac{\partial\phi}{\partial t}\,\mathrm{d}x+\int_{\partial\omega(t)}(\phi\otimes\mathbf{v})\mathbf{n}_\omega\,\mathrm{d}s-\int_{\sigma(t)}[\![(\phi\otimes\mathbf{w})\mathbf{n}_\sigma]\!]\,\mathrm{d}s.$$

If we then express the second term on the right-hand side using the modified Gauss integration formula (A.2) as

$$\int_{\partial\omega(t)}(\phi\otimes\mathbf{v})\mathbf{n}_\omega\,\mathrm{d}s=\int_{\omega_-\cup\omega_+}\mathrm{div}\,(\phi\otimes\mathbf{v})\,\mathrm{d}x+\int_{\sigma(t)}[\![(\phi\otimes\mathbf{v})\mathbf{n}_\sigma]\!]\,\mathrm{d}s,$$

the identity (A.3) follows from trivial manipulation. □

Appendix B

Coupled Calculus Properties

Here we use the coupled calculus framework on the Colombeau algebra introduced in Section 4.1.4 to prove certain properties of the formalism stated in that section. The proofs are based heavily on the proofs presented by Rosinger [1987].

Theorem B.1. *Let $f_1, f_2 \in C^0(\mathbb{R}^n)$. Their usual product $f_1 \cdot f_2 \in C^0(\mathbb{R}^n)$ can be interpreted as a regular distribution $T_{f_1 \cdot f_2} \in \mathcal{D}'(\mathbb{R}^n)$. On the other hand, we can consider the generalized functions $F_1, F_2 \in \mathcal{G}(\mathbb{R}^n)$ that correspond to f_1 and f_2 respectively according to the embedding* (4.6)*. The product $F_1 \cdot F_2 \in \mathcal{G}(\mathbb{R}^n)$ in the sense of Colombeau algebra then satisfies $F_1 \cdot F_2 \Vdash T_{f_1 \cdot f_2}$.*

Proof. Denote $F_i = \overline{f}_i + \mathcal{I} \in \mathcal{G}(\mathbb{R}^n)$, $i = 1, 2$, where $\overline{f}_i$ are given by Equation (4.7), and take $\psi \in \mathcal{D}(\mathbb{R}^n)$ arbitrary. The embedding (4.4) – (4.5) along with Definition 4.8 implies

$$\int_{\mathbb{R}^n} (\psi \cdot F_1 \cdot F_2)(x)\,\mathrm{d}x = g + \mathcal{I}_0 \in \overline{\mathbb{C}},$$
$$g(\phi) = \int_{\mathbb{R}^n} \psi(x)\overline{f}_1(\phi, x)\overline{f}_2(\phi, x)\,\mathrm{d}x, \quad \forall \phi \in \Phi.$$

On the other hand, we have $T_{f_1 \cdot f_2} = f_T + \mathcal{I} \in \mathcal{G}(\mathbb{R}^n)$ with f_T given by Equation (4.9) and analogously with the previous case we can write

$$\int_{\mathbb{R}^n} (\psi \cdot T_{f_1 \cdot f_2})(x)\,\mathrm{d}x = \hat{g} + \mathcal{I}_0 \in \overline{\mathbb{C}},$$
$$\hat{g}(\phi) = \int_{\mathbb{R}^n} \psi(x) f_T(\phi, x)\,\mathrm{d}x, \quad \forall \phi \in \Phi.$$

Take $\varepsilon > 0$ and $\phi \in \Phi$ arbitrary. By definition,

$$g(\phi_\varepsilon) - \hat{g}(\phi_\varepsilon) = \int_{\mathbb{R}^n} \psi(x) \left[\left(\int_{\mathbb{R}^n} f_1(x + \varepsilon y)\phi(y)\,\mathrm{d}y \right) \left(\int_{\mathbb{R}^n} f_1(x + \varepsilon z)\phi(z)\,\mathrm{d}z \right) - \right.$$
$$\left. - \int_{\mathbb{R}^n} f_1(x + \varepsilon w) f_2(x + \varepsilon w)\phi(w)\,\mathrm{d}w \right] \mathrm{d}x.$$

If we now take the limit $\varepsilon \to 0^+$ and realize that by construction $\int_{\mathbb{R}^n} \phi = 1$, we get $g - \hat{g} \vdash 0 \in \mathbb{C}$ and the proof is complete. □

Theorem B.2. *Let $F_1, F_2 \in \mathcal{G}(\mathbb{R}^n)$, $\alpha \in \mathbb{N}_0^n$. If $F_1 \approx F_2$, then $D^\alpha F_1 \approx D^\alpha F_2$.*

Proof. Denote $F_i = f_i + \mathcal{I} \in \mathcal{G}(\mathbb{R}^n)$, $f_i \in \mathcal{A}$, $i = 1, 2$. By definition, $F_1 \approx F_2$ implies

$$\int_{\mathbb{R}^n} (\psi \cdot (F_2 - F_1))(x)\,\mathrm{d}x \vdash 0 \in \mathbb{C}, \quad \forall \psi \in \mathcal{D}(\mathbb{R}^n),$$

which translates to

$$\lim_{\varepsilon \to 0^+} \int_{\mathbb{R}^n} \psi(x)(f_2(\phi_\varepsilon, x) - f_1(\phi_\varepsilon, x))\,\mathrm{d}x = 0, \quad \forall \phi \in \Phi_m, \forall \psi \in \mathcal{D}(\mathbb{R}^n)$$

for some $m \in \mathbb{N}$.

On the other hand, $D^\alpha F_i = D^\alpha f_i + \mathcal{I} \in \mathcal{G}(\mathbb{R}^n)$, which means that we can write

$$\int_{\mathbb{R}^n} (\psi \cdot (D^\alpha F_2 - D^\alpha F_1))(x)\,\mathrm{d}x = g + \mathcal{I}_0 \in \overline{\mathbb{C}},$$

$$\begin{aligned} g(\phi) &= \int_{\mathbb{R}^n} \psi(x) D^\alpha (f_2(\phi, x) - f_1(\phi, x))\,\mathrm{d}x = \\ &= (-1)^{|\alpha|} \int_{\mathbb{R}^n} D^\alpha \psi(x)(f_2(\phi, x) - f_1(\phi, x))\,\mathrm{d}x, \quad \forall \phi \in \Phi, \forall \psi \in \mathcal{D}(\mathbb{R}^n). \end{aligned}$$

Since $D^\alpha \psi \in \mathcal{D}(\mathbb{R}^n)$, $\lim_{\varepsilon \to 0^+} g(\phi_\varepsilon) = 0$ holds, which completes the proof. □

Lemma B.3. *With the multiplication in $\mathcal{G}(\mathbb{R})$, $H^q \approx H$ holds for all $q \in \mathbb{N}$. Moreover, $qH^{q-1}\delta \approx \delta$ holds in $\mathcal{G}(\mathbb{R})$.*

Proof. The Heaviside function can be represented by the regular distribution T_H defined as

$$\langle T_h, \varphi \rangle = \int_0^{+\infty} \varphi(x)\,\mathrm{d}x, \quad \forall \varphi \in \mathcal{D}(\mathbb{R}),$$

which in view of the embedding (4.8) – (4.9) leads to its interpretation in Colombeau algebra as

$$H = h + \mathcal{I} \in \mathcal{G}(\mathbb{R}^n),$$
$$h(\phi, x) = \int_{-x}^{+\infty} \phi(y)\,\mathrm{d}y, \quad \forall \phi \in \Phi, \forall x \in \mathbb{R}.$$

Naturally, $H^q = h^q + \mathcal{I} \in \mathcal{G}(\mathbb{R}^n)$ holds.

Take $\phi \in \Phi$ and define $\chi \in C^\infty(\mathbb{R})$ by

$$\chi(x) := \int_{-\infty}^{x} \phi(y)\,\mathrm{d}y, \quad \forall x \in \mathbb{R}.$$

The above defined function χ has the following properties:

$$\lim_{x \to -\infty} \chi(x) = 0, \quad \lim_{x \to +\infty} \chi(x) = 1, \tag{B.1}$$

$$\forall x \in \mathbb{R}, \forall \varepsilon > 0: \quad h(\phi_\varepsilon, x) = 1 - \chi\left(-\frac{x}{\varepsilon}\right). \tag{B.2}$$

Let $\psi \in \mathcal{D}(\mathbb{R})$ and denote

$$\int_{-\infty}^{+\infty} (\psi \cdot (H^q - H))(x)\,\mathrm{d}x = g + \mathcal{I}_0 \in \overline{\mathbb{C}},$$

where g can be expressed using (B.2) as

$$g(\phi_\varepsilon) = \int_{-\infty}^{+\infty} \psi(x) \left\{ \left[1 - \chi\left(-\frac{x}{\varepsilon}\right)\right]^q - \left[1 - \chi\left(-\frac{x}{\varepsilon}\right)\right] \right\} \mathrm{d}x, \quad \forall \varepsilon > 0, \forall \phi \in \Phi.$$

Define $\omega_\varepsilon(x) := [1-\chi(-x/\varepsilon)]^q - [1-\chi(-x/\varepsilon)]$ for $\varepsilon > 0$ and $x \in \mathbb{R}$ arbitrary. It follows from (B.1) that

$$\lim_{\varepsilon\to 0^+} \omega_\varepsilon(x) = \begin{cases} 0, & x \neq 0, \\ [1-\chi(0)]^q - [1-\chi(0)], & x = 0. \end{cases}$$

It is also clear that $|\omega_\varepsilon(x)| \leq (1+M)^q + (1+M)$ for all $x \in \mathbb{R}$, where $M := \int_{\mathbb{R}} |\phi(y)|\,\mathrm{d}y < +\infty$. Finally, the Lebesgue bounded convergence theorem can be used to show that $\lim_{\varepsilon\to 0^+} g(\phi_\varepsilon) = 0$, which then leads to the conclusion $H^q \approx H$.

In view of Theorem B.2, we can take the derivative of the above identity and obtain $qH^{q-1}\cdot\delta \approx \delta$ immediately. □

For the purposes of the proof of the next lemma, recall the following property of distributions (cf. [Rosinger, 1987, p. 85]). For a fixed distribution $T \in \mathcal{D}'(\mathbb{R}^n)$, the integral of the product $\psi T \in \mathcal{D}'(\mathbb{R}^n)$, $\psi \in \mathcal{D}(\mathbb{R}^n)$, can be defined as

$$\int_{\mathbb{R}^n} (\psi T)(x)\,\mathrm{d}x = T(\psi) \in \mathbb{C}, \quad \forall \psi \in \mathcal{D}(\mathbb{R}^n). \tag{B.3}$$

Lemma B.4. *There exists no distribution $T \in \mathcal{D}'(\mathbb{R})$ satisfying $\delta^2 \Vdash T$.*

Proof. Take any $\psi \in \mathcal{D}(\mathbb{R})$. By definition,

$$\begin{aligned} \int_{\mathbb{R}} (\psi\cdot\delta^2)(x)\,\mathrm{d}x &= f + \mathcal{I}_0 \in \overline{\mathbb{C}}, \\ f(\phi) &= \int_{\mathbb{R}} \psi(x)\phi^2(-x)\,\mathrm{d}x, \qquad \forall \phi \in \Phi, \\ f(\phi_\varepsilon) &= \frac{1}{\varepsilon}\int_{\mathbb{R}} \psi(-\varepsilon y)\phi^2(y)\,\mathrm{d}y, \qquad \forall \phi \in \Phi,\ \forall \varepsilon > 0. \end{aligned}$$

Assume that there exists $T \in \mathcal{D}'(\mathbb{R})$ such that $\delta^2 \Vdash T$. Equation (B.3) would then imply

$$\lim_{\varepsilon\to 0^+} \frac{1}{\varepsilon}\int_{\mathbb{R}} \psi(-\varepsilon y)\phi^2(y)\,\mathrm{d}y = T(\psi), \quad \forall \psi \in \mathcal{D}(\mathbb{R}),$$

which is clearly absurd due to both ψ and ϕ being bounded and compactly supported and $1/\varepsilon$ diverging to $+\infty$ in the limit. □

Lemma B.5. *The equivalence in the sense of association is not compatible with multiplication of generalized functions.*

Illustration of the incompatibility. Let $q, r \in \mathbb{N}$. We already know from Lemma B.3 that the identities

$$H^q \approx H, \quad (r+1)H^r\cdot\delta \approx \delta,$$

hold in $\mathcal{G}(\mathbb{R})$. If we now take the product of the left-hand sides of these identities we get, assuming multiplication compatibility,

$$(r+1)H^{q+r}\cdot\delta \approx \frac{r+1}{q+r+1}\delta,$$

whereas the product of the right hand sides yields $H\cdot\delta \approx \frac{1}{2}\delta$. For $q \neq r+1$, this clearly leads to a contradiction.

It is therefore evident that

$$H^q\cdot(r+1)H^r\cdot\delta \not\approx H\cdot\delta$$

unless $q = r+1$. □

The next result is a variation on a fundamental algebraic identity in $\mathcal{G}(\mathbb{R})$ proved by [Průša and Rajagopal, 2016, Lemma 8] that is crucial to the derivation of jump conditions in the formalism of Colombeau algebra.

Lemma B.6. *Let $F_i = f_i \in C^0(\mathbb{R}) \subset \mathcal{G}(\mathbb{R})$, $i = 1, 2, 3$, in the sense of embedding (4.6). Then*

$$F_1 \cdot H_- + F_2 \cdot H_+ + F_3 \cdot \delta \approx 0 \quad \text{in } \mathcal{G}(\mathbb{R}) \tag{B.4}$$

holds if and only if

(i) $f_1 \equiv 0$ *on* $(-\infty, 0]$,

(ii) $f_2 \equiv 0$ *on* $[0, +\infty)$,

(iii) $f_3(0) = 0$.

Proof. According to the embedding (4.6) – (4.7), we can write for $i = 1, 2, 3$

$$F_i = \overline{f}_i + \mathcal{I} \in \mathcal{G}(\mathbb{R}), \qquad \overline{f}_i(\phi, x) = \int_{-\infty}^{+\infty} f_i(x+y)\phi(y)\,\mathrm{d}y, \qquad \forall \phi \in \Phi,\ \forall x \in \mathbb{R}.$$

Next, if we interpret H_-, H_+ as their corresponding regular distributions, the embedding (4.8) – (4.9) yields

$$\begin{aligned}
H_- = h_- + \mathcal{I} \in \mathcal{G}(\mathbb{R}), &\qquad h_-(\phi, x) = \int_{-\infty}^{-x} \phi(y)\,\mathrm{d}y, &&\forall \phi \in \Phi,\ \forall x \in \mathbb{R},\\
H_+ = h_+ + \mathcal{I} \in \mathcal{G}(\mathbb{R}), &\qquad h_+(\phi, x) = \int_{-x}^{+\infty} \phi(y)\,\mathrm{d}y, &&\forall \phi \in \Phi,\ \forall x \in \mathbb{R},\\
\delta = g + \mathcal{I} \in \mathcal{G}(\mathbb{R}), &\qquad g(\phi, x) = \phi(-x), &&\forall \phi \in \Phi,\ \forall x \in \mathbb{R}.
\end{aligned}$$

Equation (B.4) is by definition equivalent to

$$\begin{aligned}
\lim_{\varepsilon \to 0^+} \int_{-\infty}^{+\infty} \Bigg[&\left(\int_{-\infty}^{+\infty} f_1(x+y)\phi_\varepsilon(y)\,\mathrm{d}y \right) \left(\int_{-\infty}^{-x} \phi_\varepsilon(y)\,\mathrm{d}y \right) + \\
&+ \left(\int_{-\infty}^{+\infty} f_2(x+y)\phi_\varepsilon(y)\,\mathrm{d}y \right) \left(\int_{-x}^{+\infty} \phi_\varepsilon(y)\,\mathrm{d}y \right) + \\
&+ \left(\int_{-\infty}^{+\infty} f_3(x+y)\phi_\varepsilon(y)\,\mathrm{d}y \right) \phi_\varepsilon(-x) \Bigg] \psi(x)\,\mathrm{d}x = 0, \quad \forall \psi \in \mathcal{D}(\mathbb{R}).
\end{aligned}$$

We proceed by investigating behaviors of individual integrals in the limit $\varepsilon \to 0^+$. It follows from trivial manipulations and properties of ϕ that for $i = 1, 2, 3$

$$\begin{aligned}
\lim_{\varepsilon \to 0^+} \int_{-\infty}^{+\infty} f_i(x+y)\phi_\varepsilon(y)\,\mathrm{d}y &= \lim_{\varepsilon \to 0^+} \int_{-\infty}^{+\infty} f_i(x+y)\phi\left(\frac{y}{\varepsilon}\right)\frac{\mathrm{d}y}{\varepsilon} = \\
&= \lim_{\varepsilon \to 0^+} \int_{-\infty}^{+\infty} f_i(x+\varepsilon z)\phi(z)\,\mathrm{d}z = f_i(x), \quad \forall \phi \in \Phi,\ \forall x \in \mathbb{R}
\end{aligned}$$

holds. Similarly,

$$\lim_{\varepsilon\to 0^+}\int_{-\infty}^{-x}\phi_\varepsilon(y)\,\mathrm{d}y=\lim_{\varepsilon\to 0^+}\int_{-\infty}^{-x/\varepsilon}\phi(z)\,\mathrm{d}z=\begin{cases}1, & x<0,\\ \displaystyle\int_{-\infty}^{0}\phi(z)\,\mathrm{d}z, & x=0,\\ 0, & x>0,\end{cases}$$

$$\lim_{\varepsilon\to 0^+}\int_{-x}^{+\infty}\phi_\varepsilon(y)\,\mathrm{d}y=\lim_{\varepsilon\to 0^+}\int_{-x/\varepsilon}^{+\infty}\phi(z)\,\mathrm{d}z=\begin{cases}0, & x<0,\\ \displaystyle\int_{0}^{+\infty}\phi(z)\,\mathrm{d}z, & x=0,\\ 1, & x>0.\end{cases}$$

This means that the limits of the three terms in the sum can be evaluated individually as

$$\lim_{\varepsilon\to 0^+}\left(\int_{-\infty}^{+\infty}f_1(x+y)\phi_\varepsilon(y)\,\mathrm{d}y\right)\left(\int_{-\infty}^{-x}\phi_\varepsilon(y)\,\mathrm{d}y\right)\psi(x)\,\mathrm{d}x=\int_{-\infty}^{0}f_1(x)\psi(x)\,\mathrm{d}x,$$

$$\lim_{\varepsilon\to 0^+}\left(\int_{-\infty}^{+\infty}f_2(x+y)\phi_\varepsilon(y)\,\mathrm{d}y\right)\left(\int_{-x}^{+\infty}\phi_\varepsilon(y)\,\mathrm{d}y\right)\psi(x)\,\mathrm{d}x=\int_{0}^{+\infty}f_2(x)\psi(x)\,\mathrm{d}x,$$

$$\begin{aligned}&\lim_{\varepsilon\to 0^+}\left(\int_{-\infty}^{+\infty}f_3(x+y)\phi_\varepsilon(y)\,\mathrm{d}y\right)\phi_\varepsilon(-x)\psi(x)\,\mathrm{d}x=\\ &\qquad=\lim_{\varepsilon\to 0^+}\left(\int_{-\infty}^{+\infty}f_3(x+\varepsilon z)\phi(z)\,\mathrm{d}z\right)\phi\left(-\frac{x}{\varepsilon}\right)\psi(x)\frac{\mathrm{d}x}{\varepsilon}=\\ &\quad=\lim_{\varepsilon\to 0^+}\left(\int_{-\infty}^{+\infty}f_3(\varepsilon(z-w))\phi(z)\,\mathrm{d}z\right)\phi(w)\,\psi(-\varepsilon w)\,\mathrm{d}w=f_3(0)\psi(0).\end{aligned}$$

In total, Equation (B.4) is equivalent to

$$\int_{-\infty}^{0}f_1(x)\psi(x)\,\mathrm{d}x+\int_{0}^{+\infty}f_2(x)\psi(x)\,\mathrm{d}x+f_3(0)\psi(0)=0,\quad\forall\psi\in\mathcal{D}(\mathbb{R}),$$

which is then equivalent to

$$f_1\equiv 0\text{ on }(-\infty,0],\quad f_2\equiv 0\text{ on }[0,+\infty),\quad f_3(0)=0,$$

and the proof is complete. □